STRUCTURE AND OPTICAL ABSORPTION PROPERTIES OF DYES EXTRACTED FROM SELECTED PLANT MATERIALS FOR DYE SENSITIZED SOLAR CELLS

BY

TIBENKANA MOHAMMAD

19/U/GMSP/18931/PD

A DISSERTATION SUBMITTED TO THE DIRECTORATE OF RESEARCH AND GRADUATE TRAINING IN PARTIAL FULFILLMENT OF THE REQUIREMENTS FOR THE AWARD OF THE DEGREE OF MASTER OF SCIENCE IN PHYSICS OF KYAMBOGO UNIVERSITY

NOVEMBER 2023

DECLARATION

I TIBENKANA MOHAMMAD declare that this is my own original work and has not been presented to any other University or Institution of Higher Education for similar or any other degree award.

Signature: ……. Date: …….

APPROVAL

The undersigned certify that the research dissertation entitled **"Structure and optical absorption properties of dyes extracted from selected plant materials for dye sensitized solar cells"** was developed by TIBENKANA MOHAMMAD and is hereby duly approved for presentation to the Directorate of Research and Graduate Training and Senate of Kyambogo University.

Dr. Emma Panzi Mukhokosi

Department of Physics, Kyambogo University, Kampala-Uganda

Signature: ……. Date: ……

(Principal Supervisor)

Dr. Michael Okullo

Department of Physics, Kyambogo University, Kampala-Uganda

Signature: ……. Date: ……..

(Co-supervisor)

DEDICATION

I dedicate this research dissertation to my beloved parents for their endless support and prayers. May the good Lord greatly bless them.

ACKNOWLEDGEMENT

I humbly acknowledge the Lord Almighty, for the protection throughout the preparation of this research dissertation.

I dearly acknowledge the unmeasurable efforts and support rendered by my supervisors, Dr. Emma Panzi Mukhokosi and Dr. Michael Okullo for their dedication towards my dissertation.

I am humbled to extend my sincere appreciation to all members of the department of Physics of Kyambogo University for their academic and moral support. Special thanks to Mr. Joseph Kawuki and Mr. John Balimunsahe, the laboratory technicians.

Lastly, I thank my class mates, Mr. Seba Sichone Ackim, Ms. Sayuni Frank and everyone who in one way or another played a role towards this achievement.

TABLE OF CONTENTS

ABSTRACT

Sunlight is a natural alternative renewable energy source to expensive hydroelectricity. Dye sensitized solar cells (DSSCs) are third generation solar cells which have the potential to significantly lower the cost associated with the first and second generation solar cells and they can easily be fabricated. A dye is an important component in a DSSC because it absorbs light, produces photoelectrons and facilitates processes of electron transfer to improve the efficiency of electrical energy conversion. It is important to modify the dye as an active component in DSSC for improved performance of optical absorption properties of the dye. Mixing chlorophyll and anthocyanin dyes aims to broaden the absorption wavelength range of visible light. In this study, the chemical structural and optical absorption properties of dyes extracted from selected plant materials for DSSCs were investigated. Anthocyanin dyes from hibiscus flower, chlorophyll dyes from pumpkin and sweet potato leaves and their composites were used as natural sensitizers in the fabrication of DSSCs. The extracted dye powders were characterized using Fourier Transform Infra-Red (FTIR) spectrophotometer to determine their chemical structural properties. The dye extracts and their composites were also characterized using UV-visible spectrophotometer to determine their optical absorption properties. Scanning Electron Microscopy (SEM) and Raman spectroscopy were used to determine the surface morphology and crystalline structure of TiO_2 thin film respectively. The performance of the developed cells was measured under one-sun illumination using a solar simulator (AM1.5 100 $mWcm^{-2}$). Keithley SMU-2450 was used to record the current-voltage (*I-V*) characteristics of the solar cells. The results reveal that the DSSC fabricated from sweet potato dye extracts had the best power conversion efficiency (PCE) of 0.5 % while that from a mixed dye of sweet potato leaves and hibiscus flower (SH) at a mass ratio of 1:3 gave the best PCE of 1 % with open circuit voltage (V_{oc}) of 0.47 V and short circuit current density (J_{sc}) of 62 $\mu A/cm^2$.

LIST OF FIGURES

LIST OF TABLES

CHAPTER ONE: INTRODUCTION

1.1 Background of the study

Energy is the backbone of any country's economic development. However, non-renewable energy sources like geothermal and nuclear are costly, difficult to replenish once used up, and emit greenhouse gases that harm the environment. Because non-renewable energy sources create threats to human health and environment, renewable energy sources offer a lot of potential as a source of alternative energy. In Uganda, there is a rising need for connections to hydro grid electricity. However, the cost of distribution to households is very high, which has increased the cost per unit of power, currently at U shs. 900 for a kilowatt. Hydroelectricity can be substituted with electricity from solar energy generated by solar panels. It is clean, abundant, and easily accessible (Butler et al., 2015). In-fact, the sun sends 13.6 TW of solar energy to the earth in one hour. This is greater than the annual global power consumption of 13 TW (Calogero et al., 2015). From the time Sir Albert Einstein first discovered the photoelectric phenomenon, the search for solar energy has advanced significantly (Aberle, 2009). Crystalline silicon solar panels still dominate the solar industry, with a reported efficiency of about 25% (Calogero et al., 2015). However, they are too expensive partly because of the indirect band gap nature of the silicon material and high processing costs (Green, 2005). Photovoltaic cells of the second and third generations, such as amorphous silicon solar cells, dye sensitized solar cells (DSSCs), are being studied extensively because of their potential to significantly lower the cost associated with the first generation solar cells. The dye sensitized solar cells are regarded as solid-state photovoltaic devices that mimic the process of photosynthesis in plants. They are easily processed with abundance of available resources and can be utilized as portable equipments like solar chargers, solar key boards and solar bags. In addition, DSSCs are considered appropriate for communities living off the grid. In dye sensitized solar cells, sensitizing dye is an important component. There has been a lot of interest in the development of new families of organic (synthetic) dyes. Ruthenium (II) and osmium (II) complexes have been discovered to be most efficient sensitizers (Desai et al., 2019). This is because they have interesting properties such as good absorption of photons in the visible region of the electromagnetic spectrum, long excited lifespan, and highly efficient metal-to-ligand charge transfer. However, they are

costly, contain heavy metals which have negative impact on the environment and require advanced processing methods (Singh & Nalwa, 2015). Therefore, the chemical structure and optical absorption properties of dyes extracted from plant materials need to be studied extensively in order to identify natural dyes that can substitute the synthetic dyes, bind effectively with the photoelectrode and absorb a wider range of photons in the visible region of the electromagnetic spectrum, which can further lead to better performance and stability of the DSSC. In this dissertation, dyes from hibiscus flower, pumpkin leaves, sweet potato leaves and their composites were extracted, their chemical structure and optical absorption properties were studied. The choice of plant materials was based on color pigments. Hibiscus flowers are red in colour and contain anthocyanin pigment which has a maximum optical absorption peak at ~ 530 nm, whereas pumpkin and sweet potato leaves are green in color and contain chlorophyll pigments with two optical absorption peaks at one at ~ 450 nm and another peak at ~ 650 nm. By combining anthocyanin and chlorophyll pigments, it is expected that the entire Ultra violet-Visible and Near infrared spectrum of the sun's energy will be covered and this will lead to improved power conversion efficiency of the fabricated solar cell. In addition, dye sensitized solar cells were developed and their efficiency studied. It was found that the efficiency of the composite dye from sweet potato leaf extract and hibiscus flower was 1 % higher than the rest.

1.2 Statement of the problem

Most DSSCs apply Ruthenium and Osmium based complexes as sensitizers with a highest reported efficiency of about 14 % (Desai et al., 2019). These complexes involve intricate preparation techniques, are expensive and contain environmentally non friendly heavy metals that are toxic (Singh and Nalwa, 2015) and can cause cancer to animals and humans if up taken by plants as nutrients since plants, animals and humans have a symbiotic relationship. Natural dyes from leaves, roots, flowers and tree barks have been investigated as an alternative to these synthetic complexes but until now no suitable replacement for the synthetic dye has been found (Sanjay et al., 2018). This could be due to single dye plant extracts such as wormwood with a reported efficiency of 0.9 % and purple cabbage with an efficiency of 1.47 % (Chang et al., 2013). Single dye plant extracts absorb light in narrow specific regions of the sun's energy depending on their color pigments. By mixing single dye pigments, there will be a wide range of optical absorption of the sun's energy and hence

improved power conversion efficiency of the solar cell. In this study, natural dyes from hibiscus flower, pumpkin leaves, sweet potato leaves and their composites were investigated as sensitizers in DSSCs.

1.3 Major objective of the study

To investigate the structure and optical absorption properties of dyes extracted from selected plant materials for dye sensitized solar cells.

1.4 Specific objectives of the study

To achieve the stated major objective, the specific objectives were:

(i) To investigate the structural properties of dyes extracted from hibiscus flower, pumpkin leaves and sweet potato leaves using Fourier Transform Infra-red spectroscopy.

(ii) To investigate the optical absorption properties of dyes extracted from hibiscus flower, pumpkin leaves, sweet potato leaves and their composites using UV-vis spectroscopy.

(iii) To determine the power conversion efficiency of a dye sensitized solar cells developed from hibiscus flowers, pumpkin leaves, sweet potato leaves and their composites by measuring short circuit current and open circuit voltage.

1.5 Scope of the study

This study focused on dyes extracted from leaves of sweet potato, pumpkin, hibiscus flower and their composites around Ugandan flora.

The study also focused on chemical structural and optical absorption properties of dyes extracted from leaves of pumpkin, sweet potato, hibiscus flower and their composites.

The experiments were conducted in the Physics, Biology, Chemistry laboratories of Kyambogo University and Ithemba Labs, South Africa.

1.6 Significance of the study

The study will provide detailed information about structural and optical properties of dye extracts from hibiscus flower, pumpkin leaves and sweet potato leaves for DSSC application.

Other researchers will use the information from this study for further research.

The information obtained will help in achieving the sustainable development goal numbers 4, 7 and 13 which emphasize quality education, affordable and clean energy and climatic action respectively.

CHAPTER TWO: REVIEW OF RELATED LITERATURE

2.1 Introduction

This chapter reviews the findings made by the past scholars on related studies. Solar spectrum, solar cell, dyes sensitized solar cell, and theory of various characterization approaches are also covered.

2.2 Solar spectrum

Solar light has a broad spectrum that ranges from gamma rays to radio waves, with a peak wavelength at 525 nm on the surface of the earth. This solar radiation does not reach the surface of the earth in its entirety. This is because different elements in the atmosphere hinder some of the radiation, changing the appearance of the solar spectrum as seen in Figure 2.1.

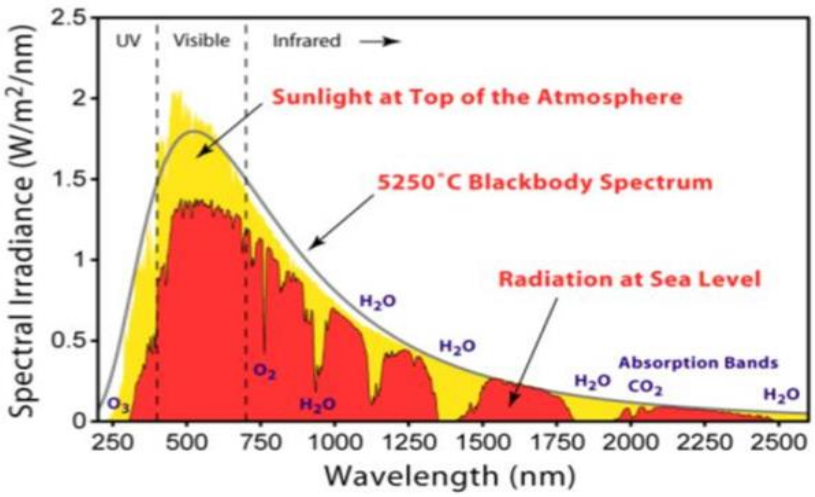

Figure 2.1: A representation of a solar spectrum on the earth's surface. Figure reproduced with permission from reference (Ramkiran et al., 2020)

2.3 Solar cell

A solar cell is a photoactive device that uses the photovoltaic effect to convert solar radiation into electrical energy (Pandikumar et al., 2019). The bending of the bands at the pn junction separates the charge carriers in the absorbing material (Kalyanasundaram, 2010). This is done when the photons are absorbed at the pn junction and then electron hole pair is generated before it is transferred to the electrodes. The internal electric fields at the junction

provide the necessary electromotive force (emf) for electric current to flow in the external circuit, resulting in power generation.

2.4 Dye sensitized solar cell

The cell is basically made up of a nanocrystalline wide band gap semiconducting electrode sensitized with a dye, a metal counter electrode and an electrolyte mediating processes of electron transfer within the cell. The electrodes contain substrates which are commonly made of glass coated with a thin layer of transparent conductive oxide (TCO) on one side (Kalyanasundaram, 2010). The transparent conductive oxides widely used for DSSCs are fluorine doped tin oxide (FTO) and indium tin oxide (ITO) (Gordon, 2000). In many optoelectronic applications, such as display and touch screens, FTO is the most commonly utilized transparent conductor (Bonaccorso et al., 2010). ITO is associated with increasing cost mainly because of rare indium substance (Paradis et al., 2015), processing requirements (Hamberg and Granqvist, 1986), challenges with patterning (Granqvist, 2007) and its sensitiveness to acidic environments (Bonaccorso et al., 2010). FTO is widely used in DSSCs because it has the best thermal stability, good conductivity and optical transparency, is less toxic, and is affordable in cost (Gordon, 2000).The photo anode commonly used is the n-type titanium dioxide (TiO_2) semiconductor with a band gap of 3.2 eV. TiO_2 thin film can be formed on the conducting side of glass substrate using techniques such as spin coating, drop casting, sol gel, electro deposition and doctor blade technique. There are three main types of nanocrystalline titanium dioxide namely; anatase, brookite and rutile and their production depend on preparation method and conditions (Reddy et al., 2001). Anatase (101) and rutile (110) are the most stable TiO_2 crystal phases (Macyk et al., 2010). The properties of anatase TiO_2 which is commonly used include; higher power density, higher charge carrier mobility and wider optical absorption range. The photo anode is sensitized with dye molecules (Memming, 1994). The molecules of the dye absorb photons of light, get oxidized and inject excited electrons into the nanostructured TiO_2. The dye should have the following characteristics to meet all the requirements:

(i) The dye's absorption spectrum should be broad to capture solar radiation, from visible spectrum to near infrared.

(ii) It should have a high molar absorptivity for efficient light harvesting.

(iii) In order to regenerate the oxidized dye molecule efficiently, the lowest occupied molecular orbitals (LUMO) level of the dye must be energetically above the semiconductor's conduction edge, while the highest occupied molecular orbitals (HOMO) level of the dye must be below the redox mediator's energy level (Meyer, 1997, Kelly and Meyer, 2001) as it is seen in Figure 2.2.

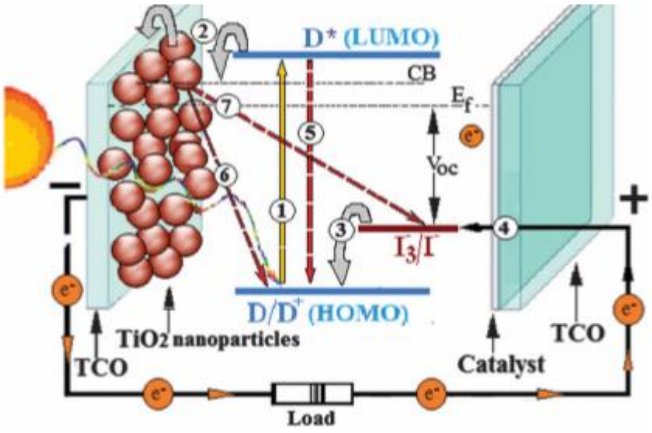

Figure 2.2: A schematic diagram showing the structure of a dye sensitized solar cell. Figure reproduced with permission from reference (Calogero et al., 2015)

The dye should be strongly anchored onto the semiconductor surface to maximize the electron injection channel. Different synthetic dyes such as ruthenium and osmium (Kuciauskas et al., 2002) and vegetable dyes (Kay and Graetzel, 1993) have been used as sensitizers in DSSCs. The most efficient synthetic dye used is Ruthenium (Ru) with a highest reported efficiency of about 14 % (Desai et al., 2019). However, Ru is rare, expensive, environmentally non friendly (Alim et al., 2022) and involves complicated preparation techniques. Organic natural dyes extracted from roots, leaves, flowers, tree barks with similar optical absorption properties can be used as a replacement to Ruthenium (II) and Osmium (II) complexes.

Various efforts have been made in extracting dyes from plant based material (Calogero et al., 2015), but until now, no suitable natural dye with properties and an efficiency similar to Ruthenium (II) and Osmium (II) complexes has been found. For example; Hao et al. used dye extracts of black rice and obtained a photoelectric conversion efficiency (PCE) of 0.327 % (Hao et al., 2006). Sirimanne et al. used anthocyanin dye in pomegranate and a PCE of

0.6 % was obtained (Sirimanne et al., 2006). Calogero and Marco took the red Sicilian orange dye and achieved a PCE of 0.66 % (Calogero and Di Marco, 2008). Most of the individual natural dyes have narrow wavelength ranges of light absorption, making the efficiency of the fabricated solar cell low. Mixing of dyes with different wavelength range of light absorption enables the dye to absorb a broader wavelength of visible light that could lead to improved efficiency of photon absorption.

The operating principle of DSSCs is summarized as follows: The photoelectrode is coated with nanocrystalline TiO_2 to give the surface area in which the dye molecules are adsorbed. When the dye molecules absorb the incident photons, they are excited from the HOMO to LUMO states;

$$S + photon \rightarrow S^* \qquad \text{(Excitation process)} \qquad 2.1$$

The dye molecule (photo sensitizer) is oxidized when an electron is transferred to the conduction band of a semiconducting material such as TiO_2 film (Kalyanasundaram, 2010).

$$S^* + TiO_2 \rightarrow e^-_{TiO_2} + S^+ \quad \text{(Injection process)} \qquad 2.2$$

The excited electron is transferred between nano particles of TiO_2 before being extracted and given as electrical energy to a load. The photoelectrode of TiO_2 and the counter electrode are usually sandwiched with the conducting sides facing each other. An electrolyte is applied between the electrodes and used as an electron mediator. The oxidized molecules of the dye are thus regenerated by receiving electrons from the ion redox mediator, which are then oxidized to tri-iodide ions.

$$S^+ + \frac{3}{2}I^- \rightarrow S + \frac{1}{2}I_3^- \quad \text{(Regeneration of the dye)} \qquad 2.3$$

The tri-iodide substitutes the internally donated electron with that from the external load and reduced back to iodide ion;

$$\frac{1}{2}I_3^- + e^- \rightarrow \frac{3}{2}I^- \text{ (Recapture reaction)} \qquad 2.4$$

The following relation for efficiency can be used to evaluate the performance of a DSSC (Grätzel, 2014);

$$\eta = \frac{V_{OC}J_{SC}FF}{P_{inc}} = \frac{P_{max}}{P_{inc}} \quad 2.5$$

Here, V_{oc} is the open-circuit voltage, J_{sc} is short-circuit current density, *FF* is the fill factor, P_{inc} is the power of the incident photons and P_{max} is maximum electrical power output. Under one sun illumination from a solar simulator (AM1.5 100 $mWcm^{-2}$), the device efficiency can be maximized by optimizing each of V_{oc}, J_{sc}, and *FF*. J_{SC} can be enhanced by using a dye sensitizer which can absorb a broad sunlight (Singh and Nalwa, 2015). The efficiency of a DSSC is highly dependent on spectrum of incident light, intensity of incident light (number of photons) and temperature of the solar cell.

2.4.1 Extraction methods and solvents

Soxhlet extraction is a continuous extraction process that uses specialised apparatus and involves a cycle of solvent reflux and percolation. Ultrasonic Assisted Extraction (UAE) uses ultrasound waves to enhance extraction process by disturbing plant cell walls. Decoction involves boiling the plant material such as roots and barks in water to speed up the extraction process. Maceration involves soaking the plant materials in a solvent such as ethanol for an extended period to extract the dye. Though relatively slow and may not extract all available dye, maceration is a simple and widely used method. The solvents used for extraction are water, ethanol, methanol, acetone and Dimethyl sulfoxide (DMSO). However, acetone and DMSO are toxic and environmentally non-friendly. Hence, ethanol can be used since it is effective for a wide range of dyes.

2.5 Theory of characterization techniques

2.5.1 Raman spectroscopy

Raman spectroscopy is an analytical technique where scattered light is used to measure the vibrational energy modes of molecules in a material such as TiO_2 and provide chemical and structural information of the material. In Raman technique, the sample is illuminated with monochromatic light, generated by a laser such as Nd; YAG at 532 nm (West, 2014). Rayleigh scatter and Raman scatter are produced. When the incident radiation interacts with an electron in the sample, the electron is promoted from the vibrational level to a virtual state of energy. This electron immediately relaxes back to the same vibrational level by losing energy equivalent to that of the incident radiation. This process leads to emission of another

photon. The released photon has the same frequency as the incident photon hence occurrence of Rayleigh scattering (West, 2014). However, electrons can relax back to a vibrational state of higher energy when losing energy. In this case, the frequency of emitted photon is higher than that of incident photon hence occurrence of Stokes Raman scattering as shown in Figure 2.3 (West, 2014).

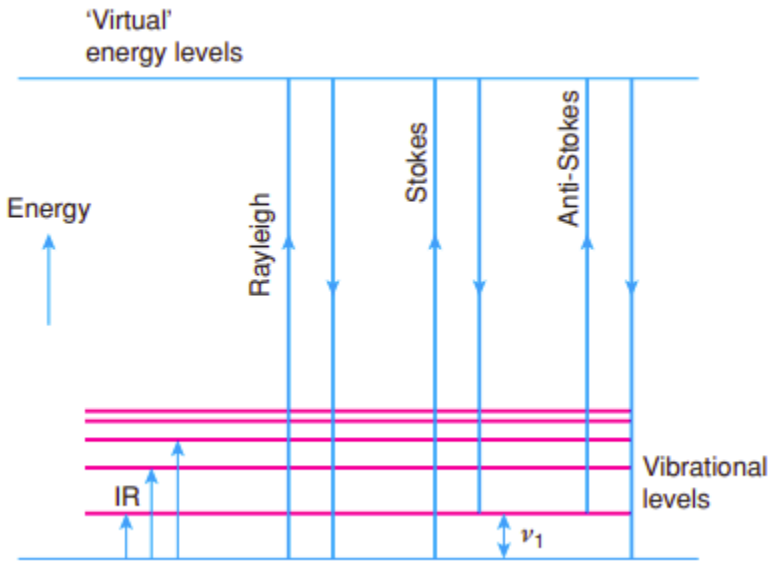

Figure 2.3: Vibrational transitions in Raman spectroscopy. Figure reproduced with permission from reference (West, 2014)

Anti-stokes Raman scattering also occurs when an electron, already in an excited state is promoted to a virtual energy state and relaxes to a ground state. In this case, the frequency of emitted photon is greater than that of incident photon (West, 2014). Raman spectra involve plots of intensity of scattering against wavenumber as shown in Figure 2.4 (Gupta et al., 2010). Raman spectra help in performing qualitative analysis. Also, intensity value of a Raman line enables determination of concentration of molecules in the sample. Hence quantitative analysis can be done.

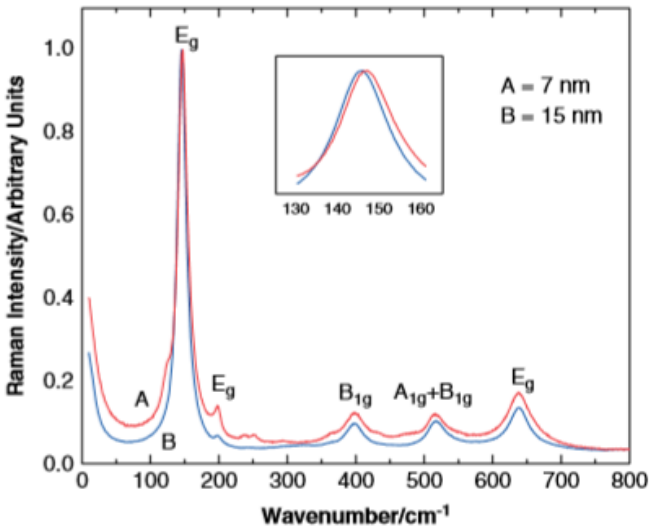

Figure 2.4: Raman spectra of TiO_2 powder of different nanocrystal sizes. Figure reproduced with permission from reference (Gupta et al., 2010)

2.5.2 Fourier Transform Infra-red (FTIR) spectroscopy

FTIR spectroscopy is a technique used to identify compounds by looking for functional groups that are contained in them. To break it down, Fourier Transform (FT) stands for a mathematical technique that takes raw data and converts it with the help of a computer, into meaningful spectra. On the other hand, IR part stands for Infra-red spectroscopy which is the type of light that this instrument uses as it interacts with the compounds. Figure 2.5 shows a schematic representation of FTIR spectrometer and how light from the source reaches different parts of the instrument as it interacts with the compounds. The frequency of incident radiation is regulated in the IR technique, and the radiation absorbed or transmitted by the sample is determined. Because the amount of absorbed energy promotes the local functional group for absorption to a higher vibrational level, the process is rather easy (Abou-Ras et al., 2016).

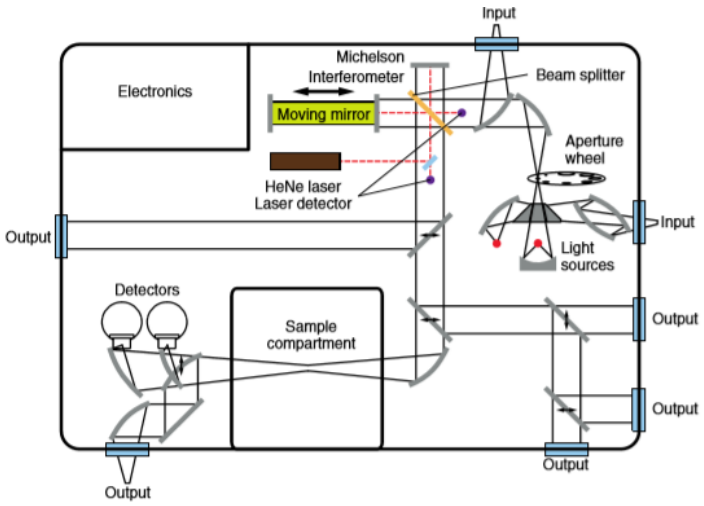

Figure 2.5: A schematic representation of FTIR spectrometer. Figure reproduced with permission from reference (Abou-Ras et al., 2016)

2.5.3 Scanning electron microscopy

Scanning electron microscopy (SEM) is a technique used to obtain high-resolution images of surfaces of materials such as TiO_2 and study their morphology. The electron gun concentrates electrons onto the sample surface. The beam of electrons then scans the sample, detecting the produced signals. The electron beam has a penetration depth of up to 1 µm (West, 2014). Imaging in the SEM must be carried out under a vacuum since electrons cannot travel through air. As electrons strike the sample, the back scattered electrons can escape from a thicker region of the sample provided they avoid secondary collisions after the initial back-scattering event as shown in Figure 2.6.

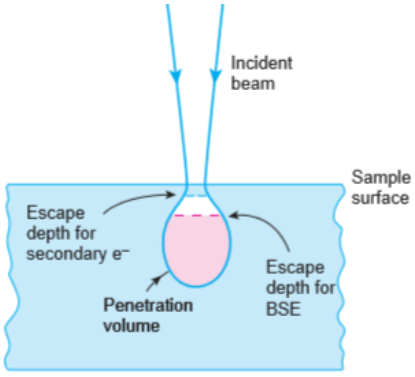

Figure 2.6: Penetration and escape depth in SEM. Figure reproduced with permission from reference (West, 2014)

Because the released radiation (x-rays and visible light) has significantly less energy than the incident beam, the escape depth is less. Some of the electrons incident on the sample penetrate deeper, lose energy to lattice vibrations and are unable to escape. In SEM, the incident electrons are unable to penetrate the sample completely. The lower limit of resolution with SEM instruments is about 100 Å. When electrons in the SEM strike the sample, particles and radiations with a wide range of energies, arising from many processes as shown in Figure 2.7, can be detected. These include secondary electrons, arising from absorption and re-emission processes, diffracted electrons, Auger electrons of characteristic energies, x-rays of both characteristic and white radiations.

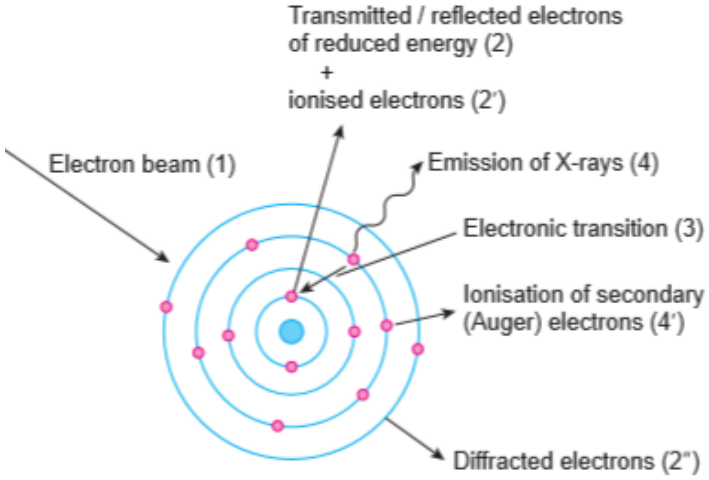

Figure 2.7: Processes that occur on bombarding a sample with electrons. Figure reproduced with permission from reference (West, 2014)

2.5.4 UV-Vis spectrophotometer

A UV-Vis spectrophotometer is used to obtain absorption peaks. It has the following fundamental components; a light source usually covered with quartz in order to transmit short wavelength of UV radiation, monochromator which is used to produce a beam of single wavelength from a radiation provided by the light source (Evans, 2004). Spectrophotometers also consist of sample holders with cuvettes that contain solutions of substance being examined and electronic detectors that are used to measure and compare intensity of light beams that go through the sample. Figure 2.8 shows the fundamental components of the spectrophotometer as discussed above.

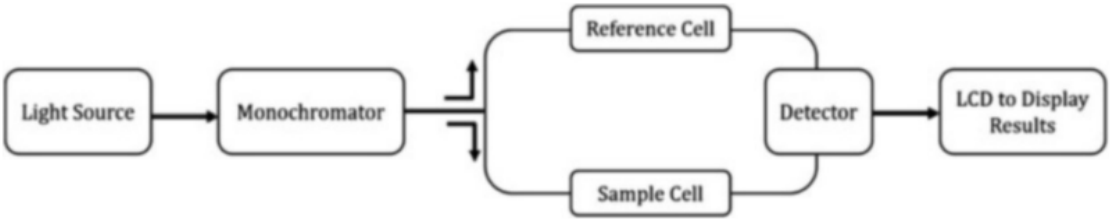

Figure 2.8: A schematic diagram of UV-visible spectrophotometer. Figure reproduced with permission from reference (Akash et al., 2020)

The graph in Figure 2.9 shows an example of visible range absorption spectrum.

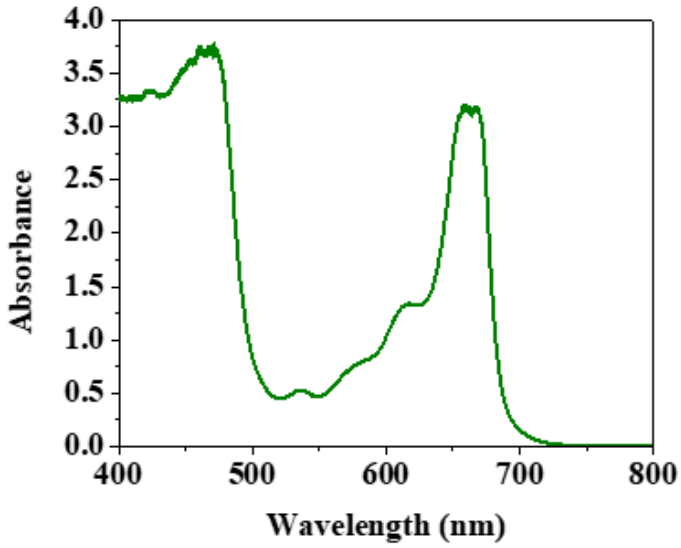

Figure 2.9: UV-visible absorption spectrum of dyes

2.5.5 Solar simulator

A solar simulator is a device that uses a light source to simulate natural sunshine in terms of intensity and spectral composition (Wang and Laumert, 2014). It is utilized for a variety of applications including testing, calibrating, and characterizing solar cells. Figure 2.11 shows a solar simulator which usually consists of three major components; light source(s) and associated power supply, any optics and filters for modifying the output beam of light to meet the requirements and necessary control units to operate the simulator.

Figure 2.10: A solar simulator (Photo was obtained from the Physics laboratory of Kyambogo University)

The spectral composition usually used for commercial solar simulators is the air mass AM1.5 (Committee, 2012). The AM1.5 spectral composition is shown in Figure 2.11.

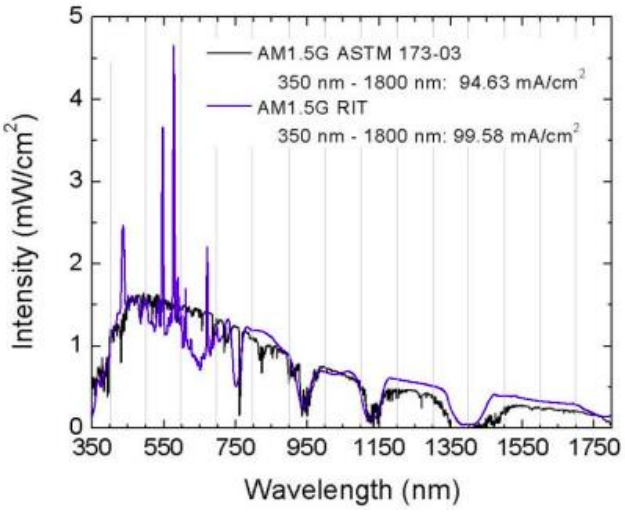

Figure 2.11: The AM1.5 spectral composition. Figure reproduced with permission from reference (Polly et al., 2011)

CHAPTER THREE: METHODOLOGY

3.1 Introduction

This chapter discusses the materials that were used, extraction of dyes from hibiscus flower, pumpkin leaves, sweet potato leaves, dye composites of hibiscus flower and pumpkin leaves, hibiscus flower and sweet potato leaves. It further discusses the preparation procedures of TiO_2 thin films on FTO substrate (photo anode) and dye adsorption, the preparation of platinum on FTO substrate (counter electrode), preparation of liquid electrolyte, determination of structural properties of dyes extracted from hibiscus flower, pumpkin leaves and sweet potato leaves, determination of optical absorption properties of dyes extracted from hibiscus flower, pumpkin leaves, sweet potato leaves and their composites, characterization of TiO_2 thin films, fabrication and testing of DSSC, determination of power conversion efficiency of a DSSC developed from hibiscus flower, pumpkin leaves, sweet potato leaves and their composites, research design, safety measures and precautions.

3.2 Materials

The materials used to extract the dyes were pumpkin (*Cucurbita maxima*) leaves, sweet potato (*Ipomoea batatas*) leaves, hibiscus (*rosa-sinensis*) flowers and ethanol. Distilled water, oven, mortar and pestle, analytical balance, measuring cylinder, amber bottles, incubator, Whatman filter paper and stickers were also used. The plant leaves were collected from Naalya town in Wakiso district. Ethanol of 96% purity was purchased from Griffchem. Fluorine doped tin oxide (FTO) substrates were used (purchased from Sigma Aldrich, sheet resistance $\sim 20\ \Omega/sq$). TiO_2 and platinum (Sigma Aldrich) were used as photo anode and counter electrode respectively. Iodide/tri-iodide (precursors from Sigma Aldrich) was used as the electrolyte. The other materials included multimeter, mobile pipette, furnace, hexa-chloroplatinic powder, iso-propyl alcohol and binder clips.

3.2.1 Extraction of dyes from hibiscus flowers and leaves of pumpkin and sweet potato.

The plant materials were cleaned with distilled water to remove any impurities on the sample. The materials were then dried in an oven for 24 hours at 60 ^{0}C. This temperature preserves the color pigments and does not degrade the dye. A mortar and pestle were used to crush the dried leaves into powder form. 10 g of pumpkin powder were dissolved in 50 ml of ethanol in an amber bottle to give a concentration of 0.2 g/ml. Similar procedures were followed for dye

extraction from sweet potato leaves. 20 g of hibiscus powder were dispersed in 100 ml of ethanol in an amber bottle to give a concentration of 0.2 g/ml. The solutions were kept in the dark for 24 hours at room temperature for a desired color pigment to be extracted. Due to the complexity of extracting dye solutions from hibiscus, the solution was warmed at 60 ^{0}C in an incubator set at 150 rpm for 10 minutes and then kept for one week to allow maceration. The solutions were filtered using Whatman filter paper (Cat No 1001 125) and kept in amber bottles in a dark environment for characterization and further use.

3.2.2 Development of composites

Using P as dyes from pumpkin leaves, S as dyes from sweet potato leaves and H as dyes from hibiscus flower, the composites were developed at three mass ratios of 3:1, 1:1 and 1:3 to optimize extraction efficiency of the dyes. Similar procedures in extraction of single dyes were followed for extraction of composites.

3.2.3 Preparation of TiO_2 thin films on FTO substrate (photo anode) and dye adsorption

TiO_2 thin films were prepared using TiO_2 powder of < 25 nm particle size (anatase phase). FTO glass substrates were cleaned thoroughly using de-ionized (DI) water and ethanol. They were then placed in a sonicator containing a combination of de-ionized water and ethanol and cleaned for 3 hours to remove any impurities on the sample. 1 g of TiO_2 powder was dispersed in 300 mg of polyethylene glycol consisting of a mixture of glacial acetic acid and double distilled water of 6 ml each. The mixture was sonicated for three hours. The edges of FTO substrate were sealed using cello tape. TiO_2 paste was drop casted on the substrate and kept for 24 hours before annealing at 300 ^{0}C in a furnace for 1 hour. The film was dipped in the dye extract for 24 hours to adsorb dye molecules. The soaked film was withdrawn from the dye, rinsed with ethanol to remove the unabsorbed dye and then used as a photo anode.

3.2.4 Development of platinum on FTO substrate (counter electrode)

FTO glass substrates of dimensions 2.5 cm × 2.5 cm were cleaned using distilled water and then isopropyl alcohol in an ultrasonic bath. The glass substrates were then left to dry under room temperature for 20 minutes. This time allows the substrates to reach a stable temperature. The edges of FTO substrate were sealed using cello tape. FTO coated surfaces of the substrates were drop casted with alcoholic solution of hexa-chloroplatinic acid prepared by dispersing 40 mg of hexa-chloroplatinic powder in 10 ml of ethanol. The samples were

kept for 24 hours to evaporate the solvent at room temperature before annealing at 300 ^{0}C for 30 minutes.

3.2.5 Preparation of liquid electrolyte

0.127 g of iodine (I_2) and 0.83 g of potassium iodide were dissolved in 10 ml of ethylene glycol placed in a clean container. The combination was stirred for 30 minutes using a glass rod and then stored in a sealed bottle (Zulkifili et al., 2015).

3.3 Determination of structural properties of dyes extracted from hibiscus flower, sweet potato and pumpkin leaves.

FTIR Spectrophotometer was used to determine chemical structure (functional groups) present in extracted dyes. This is because FTIR spectrophotometer measures absorption and transmission of infrared light by the dye and different functional groups have characteristic absorption frequencies in the infrared region allowing identification of specific material. Also, FTIR analysis is a non-destructive technique. The sample pan and the bottom of the pointer of the adjustment knob were cleaned with ethanol and soft tissue. 2 g of dye powder were then placed at the position of the prism pointer in the FTIR (SHIMADZU IRTracer-100 (EN230V)) machine. The pointer was adjusted until a click is felt in the adjustment stage. The spectrophotometer produced a beam of infra-red radiation which passes through the sample. The dye then absorbed some of the infrared radiations at certain wavenumbers in the range 4000 to 500 cm^{-1} and the others were transmitted. The amount of absorption was detected and compared. The resulting spectra as shown in Figure 3.1 were analyzed using origin software and then used to identify the chemical structure of the sample.

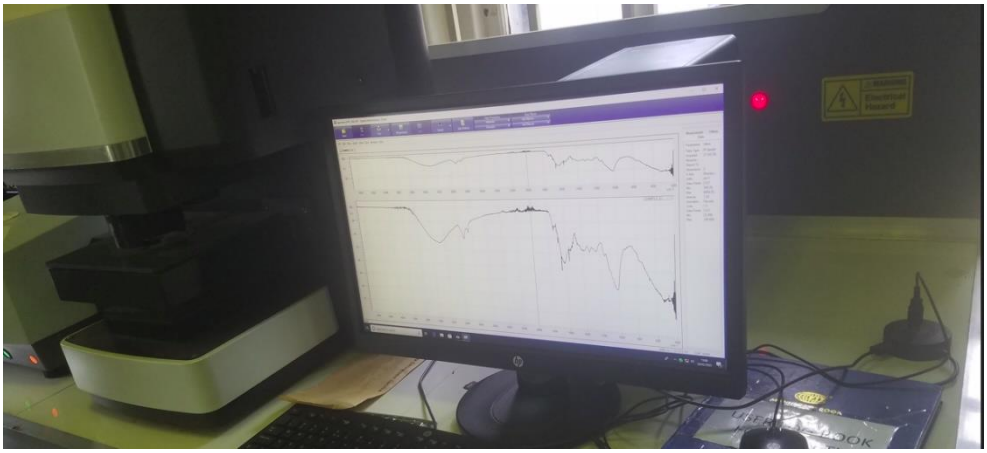

Figure 3.1: Fourier Transform Infra-Red (FTIR) spectrophotometer and FTIR spectrum measurement system (Photo was taken from government analytical laboratory, Wandegeya)

3.4 Determination of optical absorption properties of dyes extracted from hibiscus flower, pumpkin leaves, sweet potato leaves and their composites

The optical absorption properties of dye extracts were obtained using an ultra violet (UV-Vis) spectrophotometer (Genesys 10S UV-Vis). This is because dye molecules have characteristic absorption bands ranging from ultraviolet to visible regions of the electromagnetic spectrum. Two cuvettes, one containing dye solution and the other having solvent were inserted in the sample compartment of the spectrophotometer as shown in the Figure 3.2. A beam from a UV-visible light source was allowed to hit a monochromator so that a beam of single wavelength passes through it. This beam was divided into two intensity beams using a half-mirrored device. One beam went through a cuvette having a solution of the sample being investigated and the other beam passed through an identical cuvette having only the solvent. The intensities of the resulting light beams were then measured using electronic detectors and then compared. The resulting spectra were analyzed using origin software and then used to determine optical properties of the samples.

Figure 3.2: UV-Visible spectrophotometer (Photo was taken from the Chemistry laboratory of Kyambogo University)

3.5 Characterization of TiO_2 thin films

The optical absorption properties of TiO_2 thin films were obtained using an ultra violet (UV-Vis) spectrophotometer in Diffuse Reflectance Spectroscopy (DRS) format. TiO_2 thin films may have absorption features ranging from ultraviolet to visible region of the electromagnetic spectrum. Also, DRS mode is suitable for samples with a textured surface such as TiO_2 thin films. The crystalline structure of TiO_2 thin films and surface morphology of the synthesized sample were characterized using Raman spectroscopy and Scanning electron microscopy (SEM), respectively. Transmission electron microscope (TEM) was also used to determine the particle size of TiO_2 nanoparticles.

3.6 Fabrication and testing of DSSC

The dye adsorbed on TiO_2 electrode and platinum based counter electrode were sandwiched in such a way that conductive sides face each other as shown in Figure 3.3 (a). The tri-iodide/iodide (electrolyte) solution was introduced between the electrodes by capillary action. Clips were used to bind the electrodes together (Younas and Harrabi, 2020). The performance of the cells was measured under one-sun illumination from a solar simulator (AM1.5 100 $mWcm^{-2}$). Keithley SMU-2450 was used to record the current-voltage (*I-V*) characteristics of

the solar cells since it is designed to function as both voltage sources and current meters simultaneously.

Figure 3.3: (a) Fabricated DSSC (b) Solar simulator and Keithley SMU-2450

The fabricated cell was connected to Keithley using four probe and then placed below the solar simulator in such a way that the photoelectrode faces the lamp of the simulator. The sweep starts and stop voltages of keithley were set at -1 V and +1 V respectively. The step voltage and source limit current were 10 mV and 1.05 A respectively. The Keithley was then triggered to generate a graph and the data obtained was used in origin to produce *I-V* and *P-V* characteristic curves.

3.7 Determination of power conversion efficiency of a dye sensitized solar cell developed from hibiscus flowers, pumpkin leaves, sweet potato leaves and their composites

Equation 2.5 was used to determine the photovoltaic performance of the fabricated dye sensitized solar cells (DSSCs). The open circuit voltage, short circuit current density and fill factor were obtained from the *I-V* characteristic graph as shown in Figure 3.4.

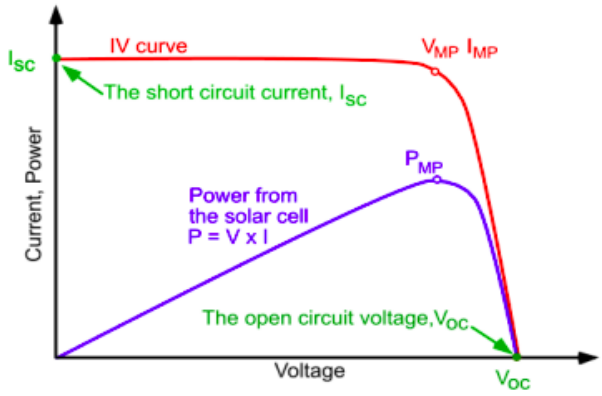

Figure 3.4: I-V and P-V characteristic curve. Figure reproduced with permission from reference (Honsberg and Bowden, 2019)

3.8 Research design

This study involved experimental method of collecting data and Figure 3.5 shows a summary of key processes involved before the fabrication of the DSSCs. The data obtained was analyzed using Origin 8.5 software.

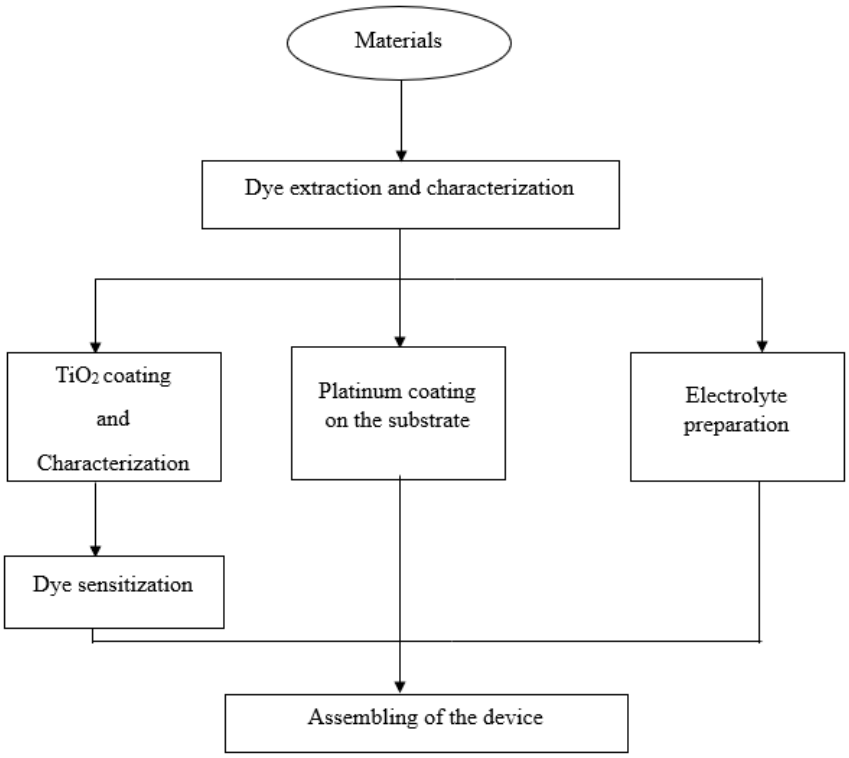

Figure 3.5: A schematic diagram showing the overall experimental design

3.9 Safety measures and precautions

The chemicals used in this study were properly labelled, stored and handled according to safety data sheets. Experiments were done while using a fume hood to minimize exposure to toxic chemicals. A proper waste disposal system for chemicals and solvents such as ethanol was done. Proper electrical safety guidelines were also followed when working with electrical equipment such as Keithley. There were also periodic inspections in the laboratory to avoid expired chemicals and equipment malfunctions.

CHAPTER FOUR: RESULTS AND DISCUSSION

4.1 Introduction

This chapter covers results and discussion of experimental results obtained. This includes; chemical structural properties of dye extracts from pumpkin leaves, sweet potato leaves and hibiscus flower, optical absorption properties of dye extracts from the same single dyes and their composites, characterization of TiO_2 thin films and power conversion efficiency of the dye sensitized solar cell developed from the plant materials.

4.2 Chemical structural properties of dyes extracted from hibiscus flower, sweet potato and pumpkin leaves (FTIR analysis)

Dyes are expected to have certain functional groups for better adsorption onto the photo-electrode thin film. The hydroxyl groups (-OH) and carbonyl groups (-CO) in chlorophyll and anthocyanin dyes make them bind effectively with the photoelectrode (Chang et al., 2013). Figure 4.1 shows the FTIR spectra of single dyes P, S and H within the wavenumber range of 4000-500 cm^{-1}. The broad absorption at wave number range 3600-3200 cm^{-1} in Figure 4.1a-b is due to O-H stretching vibration in chlorophyll dyes at a peak of about 3278 cm^{-1}. The C-H_3 and C=C alkene stretching vibrations are observed at 2924 cm^{-1} and about 1620 cm^{-1}, respectively. The broad absorption for anthocyanin at 3264 cm^{-1} in Figure 4.1 (c) corresponds to H-bond (Ezike et al., 2021). The functional groups discussed in this study agree with the chemical structure of chlorophylls and anthocyanins as shown in Figure 4.2 (Onah et al., 2020). Because both chlorophyll and anthocyanin dyes contain functional groups, they are useful as sensitizers in DSSCs (Ezike et al., 2021).

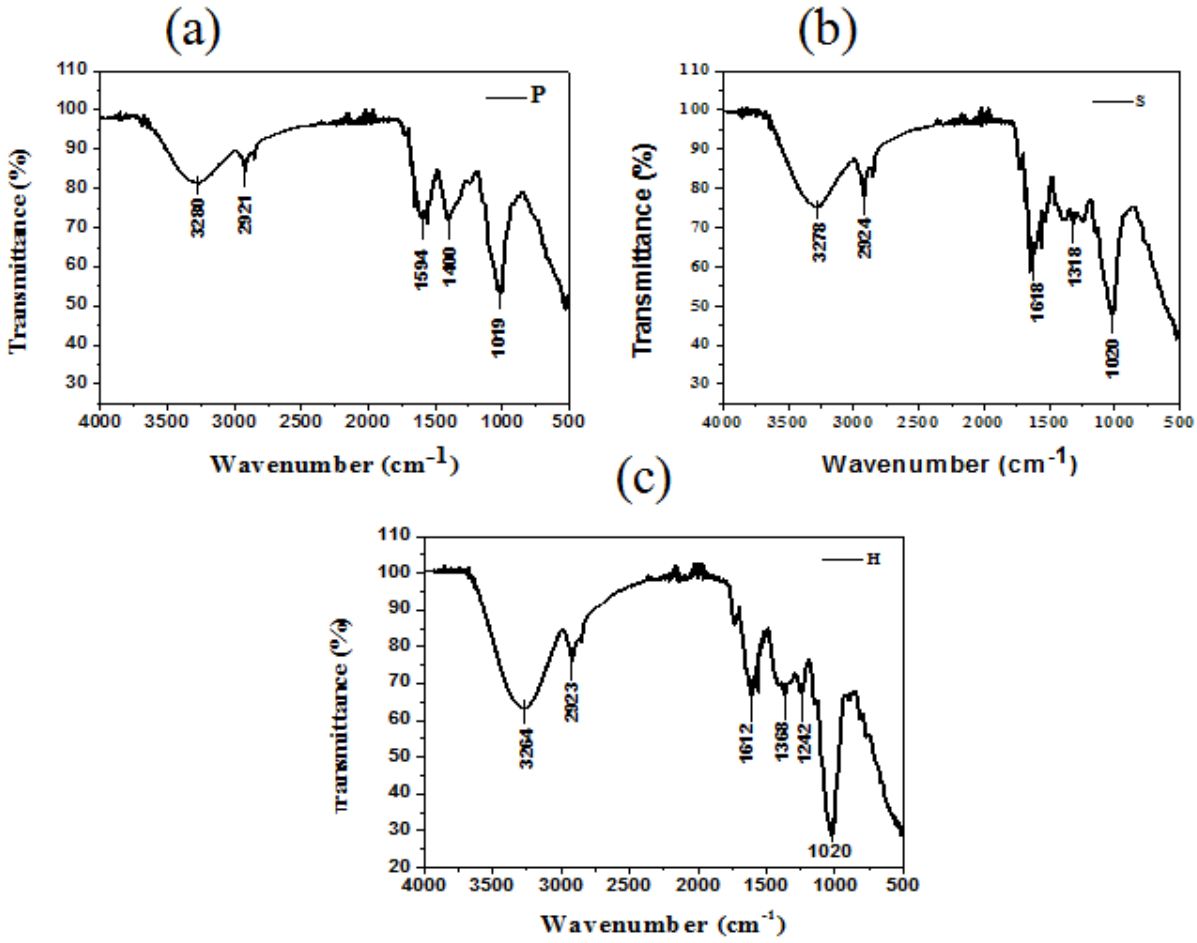

Figure 4.1: FTIR spectra for (a) pumpkin, (b) sweet potato and (c) hibiscus

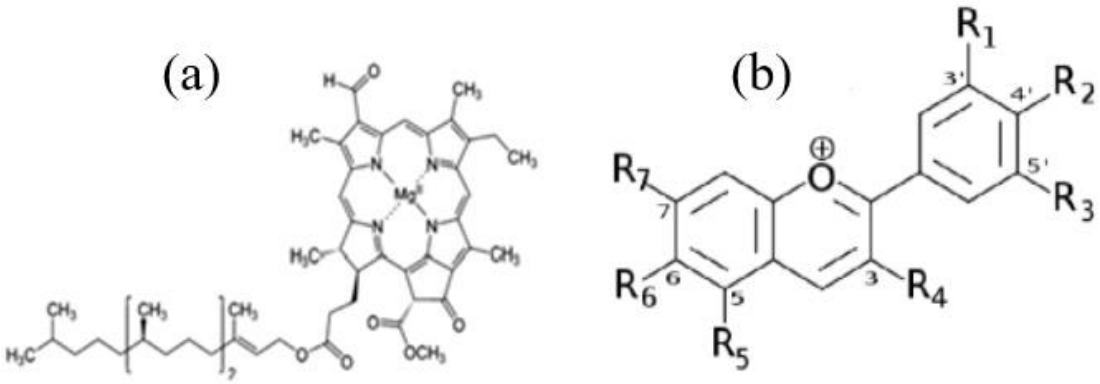

Figure 4.2: Chemical structure for (a) chlorophyll, (b) anthocyanin. Figure reproduced with permission from reference (Onah et al., 2020)

4.3 Optical absorption properties of dyes extracted from hibiscus flowers, pumpkin leaves, sweet potato leaves and their composites

4.3.1 Optical absorption properties of individual dye extracts

(a) Hibiscus

The characteristics of absorbance of hibiscus dye are shown in the Figure 4.3 which depict the results of absorption spectrum of hibiscus dye extract. The maximum absorption peak for hibiscus is observed at 525 nm. This shows that green and adjacent colors are absorbed and red in hibiscus is reflected hence presence of anthocyanin pigment in hibiscus. The absorption peak obtained is in agreement with earlier reports (Yuniati et al., 2021, Munandar et al., 2022, Zainul and Isara, 2019).

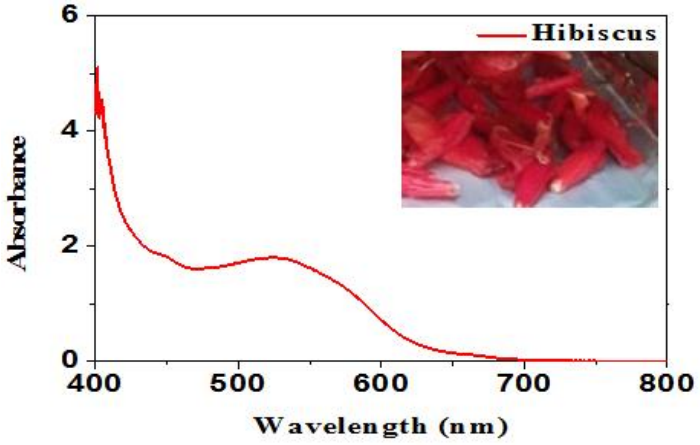

Figure 4.3: Absorption spectrum for hibiscus dye extract. The inset is a photograph of hibiscus flowers.

(b) Pumpkin

The characteristics of absorbance of pumpkin dye is shown in the Figure 4.4. The absorbance spectrum shows two maximum absorption peaks at 469 and 661 nm. This implies that colors in the blue and red region of the visible spectrum are absorbed and green color is reflected which is a characteristic of chlorophyll pigment. The maximum absorption peaks obtained correlate well with earlier reports (Clementson and Wojtasiewicz, 2019, Palupi et al., 2020).

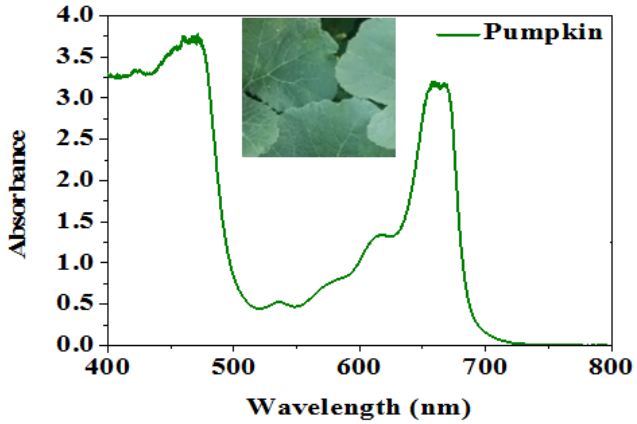

Figure 4.4: Absorption spectrum for pumpkin dye extract. The inset shows a photograph of pumpkin leaf.

(c) Sweet potato

Figure 4.5 shows the absorption spectrum for sweet potato with two maximum absorption peaks at 421 and 665 nm. This implies that colors in the blue and red region are absorbed and green color is reflected which is a characteristic of chlorophyll pigment (Lai et al., 2008, Palupi et al., 2020, Cho et al., 2014). It can be noted from the spectra that color plays a key role in light absorption.

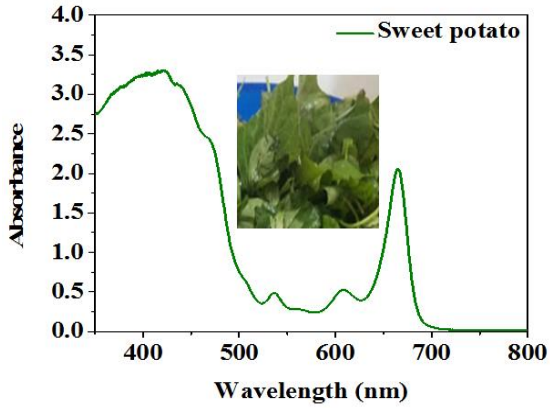

Figure 4.5: Absorption spectrum for sweet potato dye extract. The inset shows a photograph of sweet potato leaves.

4.3.2 Optical absorption properties of mixed dye extracts (composites)

Mixing of dyes can be done by using at least two extracts that possess different properties of optical absorption. Dye mixing enables the dye to absorb a broader wavelength range of visible light that could lead to improved efficiency of photon absorption. Chlorophyll and anthocyanin dyes were considered in this study since they have different absorption spectra. Therefore, they could synergize each other.

(a) Pumpkin and hibiscus mixture

Ratios of 1:1, 1:3 and 3:1 were used for this mixture. It was observed that a mixture of pumpkin and hibiscus dyes leads to absorption of photons in the green region which were previously reflected by the single chlorophyll (pumpkin) dye and also extends the absorption range of hibiscus. For this composite, there is a red shift from about 661 nm to between 663-665 nm as shown in Figure 4.6, giving a difference of 2-4 nm. The red shift is due to presence of anthocyanin and chlorophyll interaction. The slightly increased wavelength allows wide range of absorption of sun's energy which could lead to improved efficiency of a solar cell.

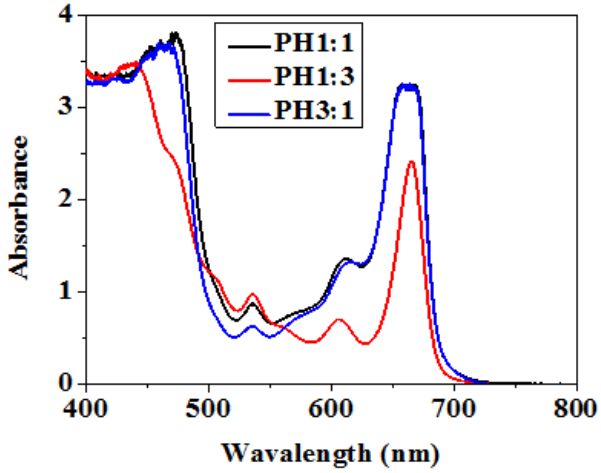

Figure 4.6: Absorption spectra of pumpkin and hibiscus mixture at different ratios

(b) Sweet potato and hibiscus mixture

Using the same ratios as in pumpkin and hibiscus mixture. It was observed that a mixture of sweet potato and hibiscus dyes leads to absorption of photons in the green region which were previously reflected by the single chlorophyll (sweet potato) dye and also extends the absorption range of hibiscus. For sweet potato and hibiscus composite in the ratio of 1:3,

there is a red shift from 665 nm to 666 nm as shown in Figure 4.7, giving a difference of 1 nm. The red shift is due to presence of anthocyanin and chlorophyll interaction. The slightly increased wavelength allows wide range of absorption of sun's energy which could lead to improved efficiency of a solar cell.

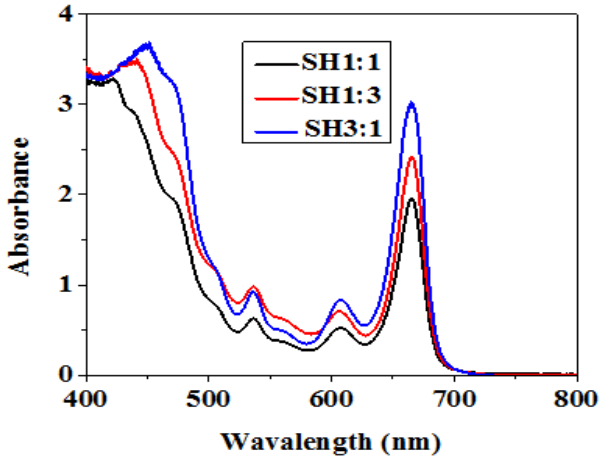

Figure 4.7: Absorption spectra for sweet potato and hibiscus mixture at different ratios

4.3.3 Band gap analysis

The band gap energy of all the samples were estimated using a Tauc plot and were calculated using classical absorption equation 4.1 (Viezbicke et al., 2015, Sumiarna and Maddu, 2016).

$$(\alpha h\upsilon)^r = A(h\upsilon - E_g) \qquad 4.1$$

where E_g represents the energy band gap, A is a constant parameter, $h\upsilon$ is energy, α is the absorption coefficient and r represents the nature of transition in the sample. In addition, $r = 2$ represents direct allowed transition, $r = \frac{1}{2}$ shows indirect allowed transition, $r = \frac{2}{3}$ for direct forbidden transitions and $r = \frac{1}{3}$ is for indirect forbidden transitions. Tauc plot has $(\alpha h\upsilon)^r$ on the vertical axis and $h\upsilon$ on the horizontal axis. After plotting, the energy gap value, E_g was obtained by extrapolating the linear part of the graph to zero.

(a) Band gap analysis of individual dyes

Figure 4.8 indicates the Tauc plot for hibiscus, pumpkin and sweet potato leaf extracts. The band gap value for hibiscus was calculated as 2.03 eV as shown in Figure 4.8 (a). This value is in accordance with what has been determined by other researchers (Saha et al., 2016).

Pumpkin and sweet potato dye extracts had two band gap values each, which were calculated as 1.82 and 2.51 eV as shown in Figure 4.8 (b) and 4.8 (c) respectively. These values correlate with what has been published by other researchers (Oktariza et al., 2018).

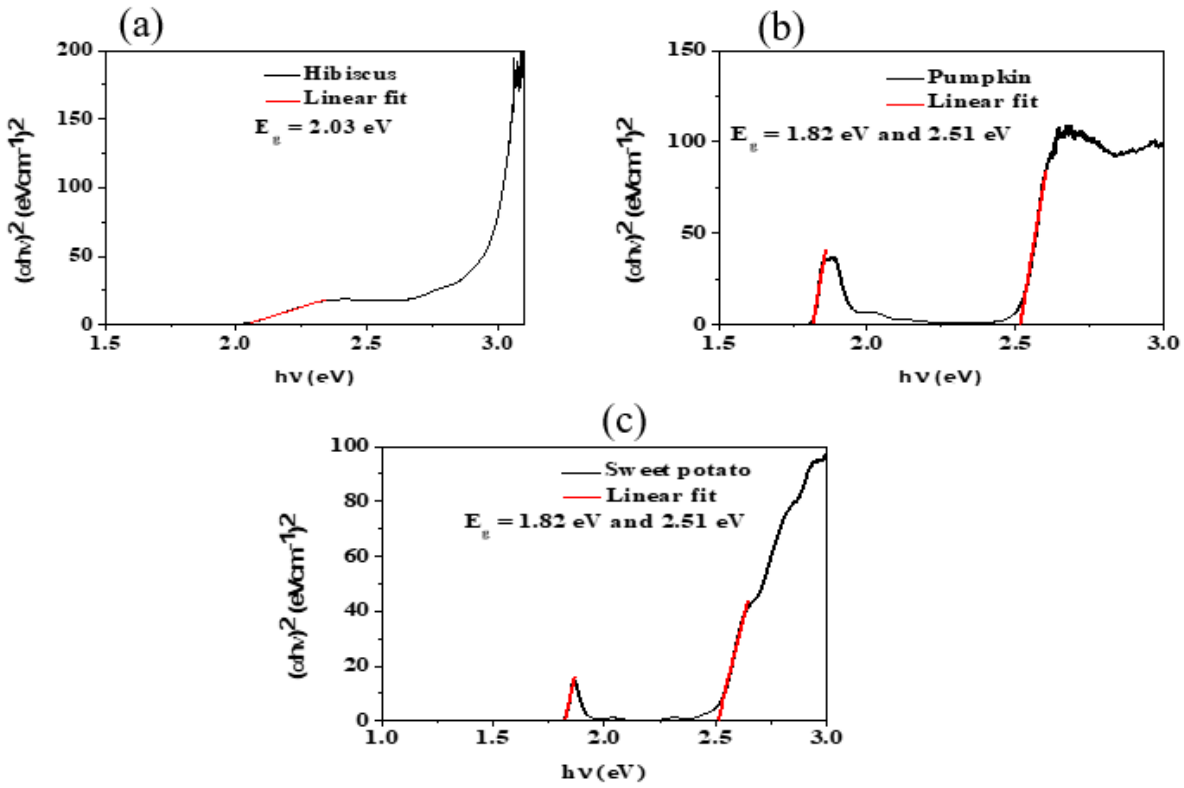

Figure 4.8: Tauc plot for (a) hibiscus, (b) pumpkin and (c) sweet potato

(b) Band gap analysis of dye composites

The band gap spectra of dye composites are shown in Figure 4.9. The band gaps for PH and SH mixture in a ratio of 1:3 are 1.98 eV for hibiscus in each mixture and 1.82 eV and 2.49 eV for pumpkin and sweet potato in the respective mixtures as shown in Figure 4.9. It was observed that energy gaps from dye mixtures were less than the band gaps of individual dyes. This is because of a better absorbance of dye composites when compared to single dyes. A combination of anthocyanin and chlorophyll dyes widens the absorption spectra and improves solar cell performance (Ezike et al., 2021).

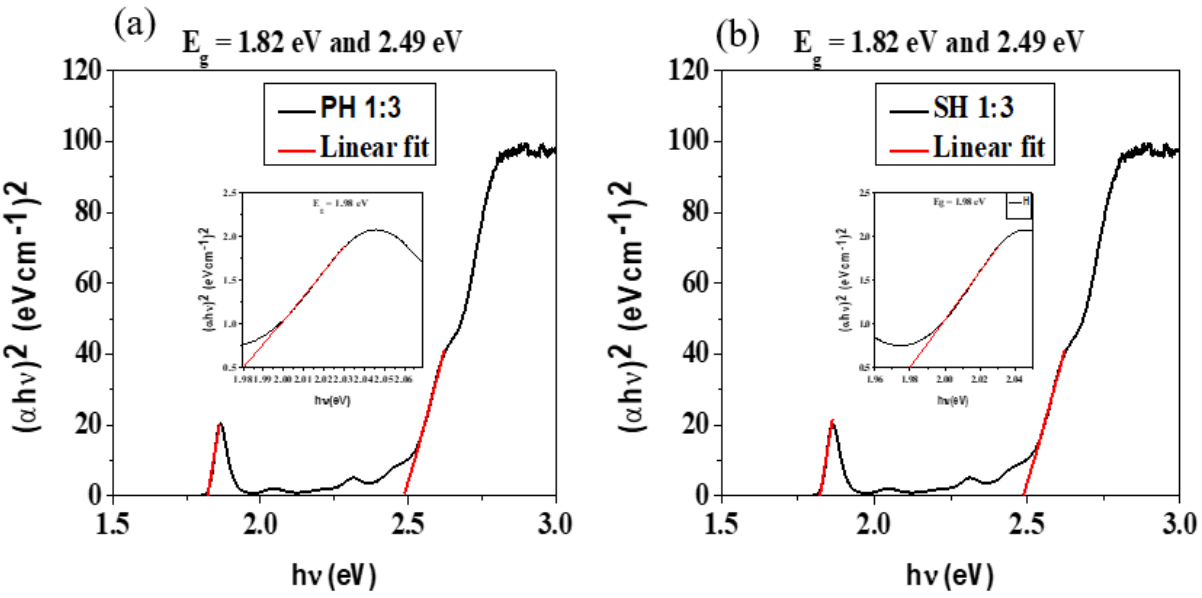

Figure 4.9: Tauc plot for (a) pumpkin and hibiscus mixture, (b) sweet potato and hibiscus mixture

4.4 Characterization of TiO_2 thin film

4.4.1 Surface morphology

The morphological features of TiO_2 thin films deposited on glass substrates were investigated using a SEM as shown in Figure 4.10. SEM image in Figure 4.10 (a) shows that particles of TiO_2 on glass are agglomerated. In addition, the particles of TiO_2 after dye adsorption in Figure 4.10 (b) are non-agglomerated and make large contact area. It could also be observed that TiO_2 is irregular and grains are spherical in shape with an average particle size of 12 ± 2 nm as illustrated in Figure 4.11 (b). The peak of Gaussian curve reveals the average particle size commonly found within the sample as shown in figure 4.11 (b).

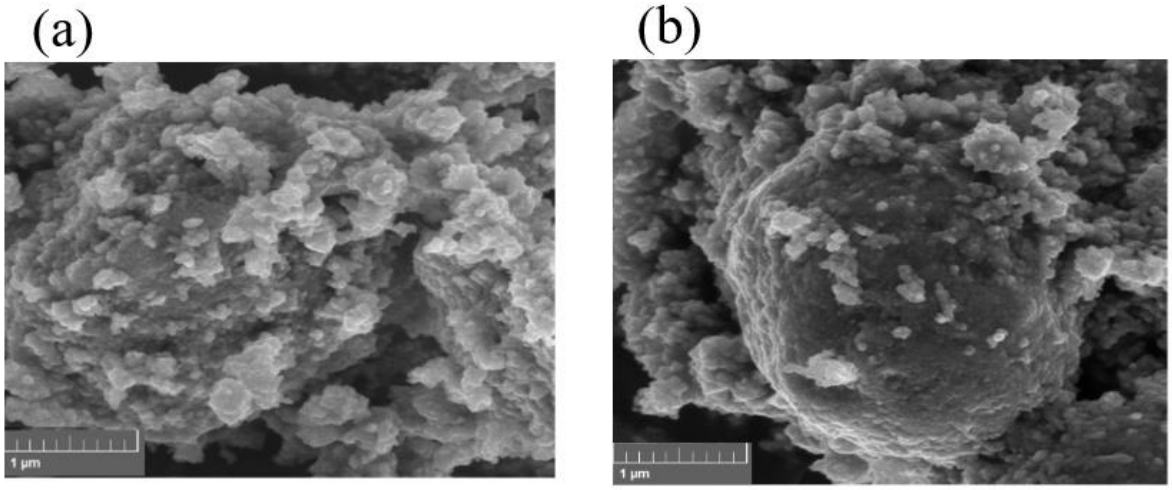

Figure 4.10: (a) SEM image for TiO_2 on glass (b) SEM image for TiO_2 after dye adsorption

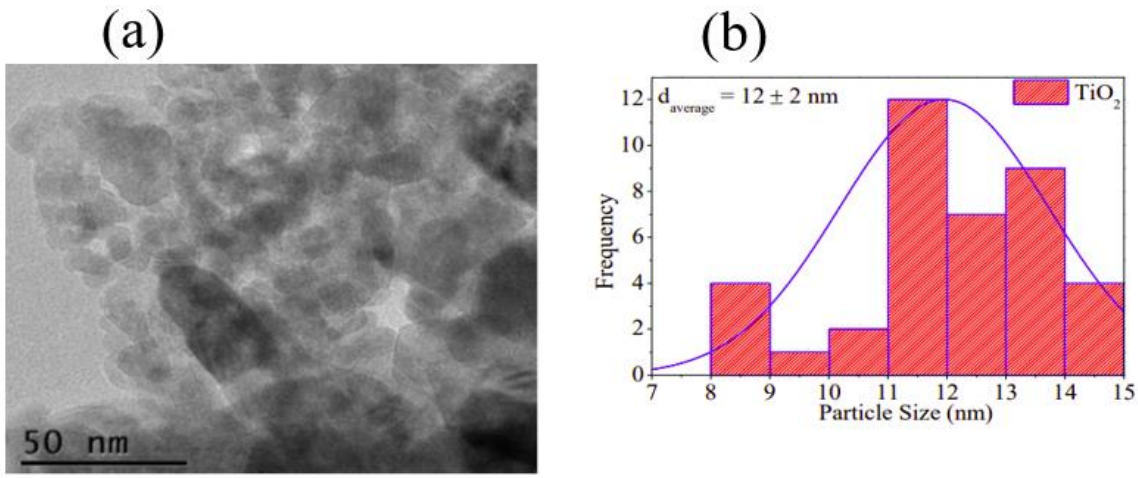

Figure 4.11: (a) TEM image for TiO_2 (b) Histogram showing particle size distribution for TiO_2

4.4.2 Structural analysis

The TiO_2 thin films were structurally analyzed using Raman spectroscopy. The results are presented in Figure 4.12. The Raman modes indicated irregular polycrystalline thin films with varying high and low modes observed at 148.6, 400.0, 520.2 and 644.0 cm^{-1}. These modes confirm the anatase form of TiO_2 in the film (Gupta et al., 2010).

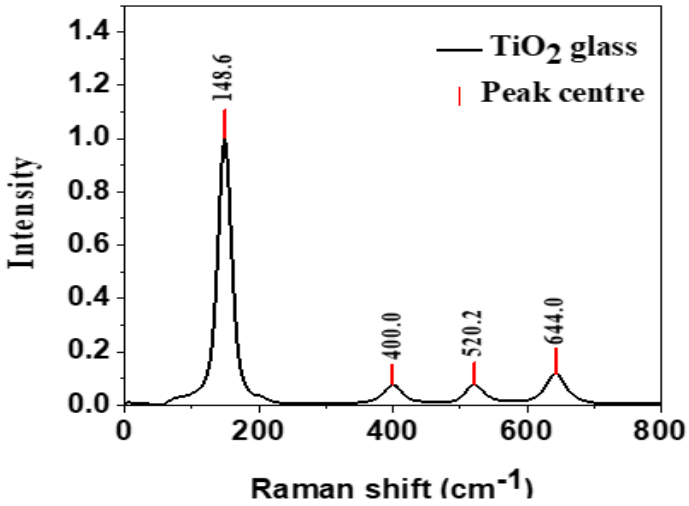

Figure 4.12: Raman spectrum for TiO_2 on glass

4.4.3 Band gap analysis of TiO_2

Kubelka munk equation 4.2 was used to calculate the band gap of TiO_2.

$$(F(R)h\upsilon)^r = A\left(h\upsilon - E_g\right) \qquad 4.2$$

Where $F(R)$ is the Kubelka munk function. From the Kubelka plot in figure 4.13, the band gap, E_g was obtained as 3.34 eV. This value correlate with what other researchers have reported about TiO_2 (Onah et al., 2020).

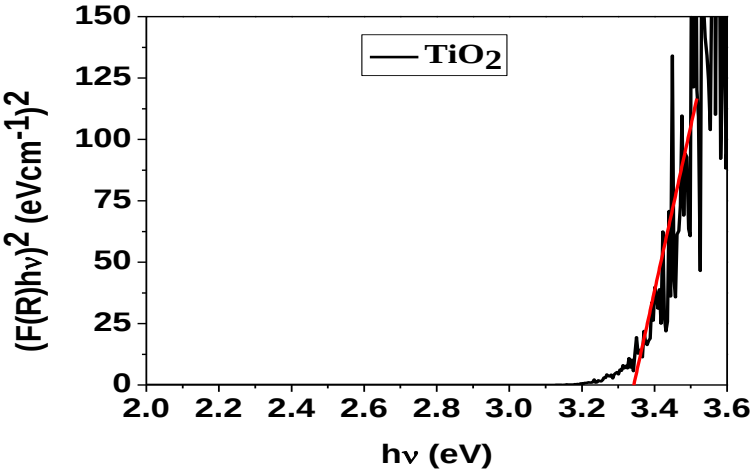

Figure 4.13: Kubelka curve of TiO_2 for direct transition

4.5 Power conversion efficiency of dye sensitized solar cell developed from hibiscus flower, pumpkin leaves, sweet potato leaves and their composites

The power conversion efficiency (PCE) of the fabricated DSSCs was determined using the expression in equation 2.5. The open circuit voltage and short circuit current density were determined from the *J-V* characteristic graph as shown in Figure 4.14 (a). For dye sensitized solar cells fabricated from individual dyes, sweet potato (S) based DSSC had a power conversion efficiency (PCE) of 0.5 % followed by pumpkin (P) with an efficiency of 0.3% and then hibiscus (H) with the least efficiency of 0.08 %. The best PCE in sweet potato (S) based DSSC is attributed to a wide range of absorption of photons in the visible region of the electromagnetic spectrum and effective binding of the dye with the photoelectrode, hence a higher short circuit current density as shown in Figure 4.14 (a) and better performance of the device. Dye sensitized solar cells fabricated from dye composites have better power conversion efficiencies than the individual dyes. This is as shown in Figure 4.15 (b). The cell based on SH (1:3) dye composite has a PCE of 1.0 % which is greater than 0.65% of PH composite based DSSC. The performance of composite based DSSCs is attributed to a mixture of chlorophyll and anthocyanin dyes which shows an increase in the absorption wavelength range as compared to the absorption wavelength range of the individual dyes, hence a better short circuit current density and improved efficiency.

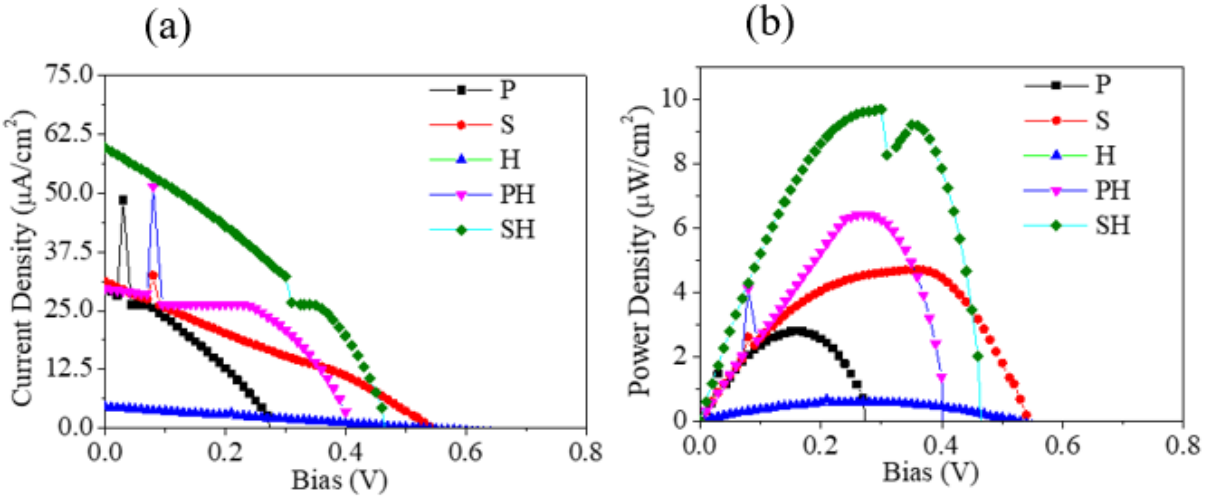

Figure 4.14: (a) J-V characteristic curve (b) P-V characteristic curve

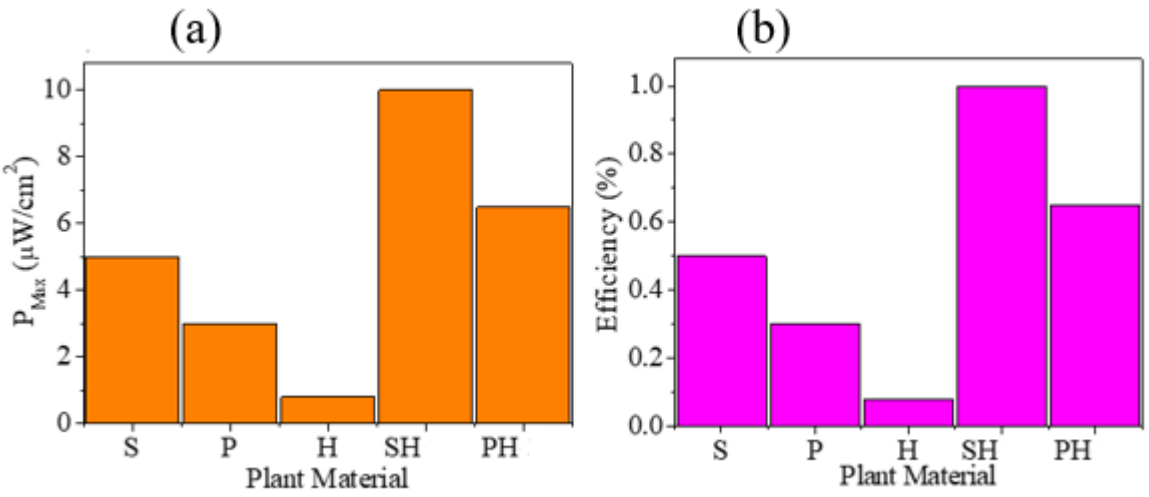

Figure 4.15: (a) Bar graph of maximum power (b) Bar graph of power conversion efficiency of plant materials

From the results obtained,it reveals that there is improved transfer of electrons to the TiO_2 photoelectrode and hence better efficiency in the dye composite based DSSCs. This could be due to presence of increased bonds of mixed dyes that bind well with the molecules of TiO_2 allowing electron transfer from the excited dye molecules to TiO_2 film. Figure 4.15 (a) and 4.15 (b) show that the individual powers and efficiencies for sweet potato and pumpkin based dye sensitized solar cells are higher than that of hibiscus. However, their combination was not considered because they have the same chlorophyll pigment, absorb photons in the same wavelength range of visible light in the electromagnetic spectrum hence could not offer a significant different result. The photoelectric performance of the developed DSSCs agree with the optical absorption property of the extracted dyes as has been observed by other researchers (Kimpa et al., 2017). Table 4.1 shows a comparison between the power conversion efficiencies (PCE) obtained in this study and literature values to further position work in this study.

Table 4.1: Power conversion efficiencies obtained in this study and different plants of similar pigments

Sample	PCE (%)	Reference
H	0.08	This work
P	0.30	This work
S	0.50	This work
PH 1:3	0.65	This work
SH 1:3	1.00	This work
Sabdariffa (Roselle)	0.0005	(Rosli et al., 2021)
Callindra haematocephata	0.06	(Maurya et al., 2016)
Pandan leaves	0.00014	(Rosli et al., 2021)
Baobab leaves	0.11	(Ndeze et al., 2021)
Carica papaya leaf and black cherry fruit (mixture)	0.56	(Ossai et al., 2021)

CHAPTER FIVE: CONCLUSION AND RECOMMENDATION

5.1 Conclusion

Three natural dyes extracted from hibiscus flowers, pumpkin leaves, sweet potato leaves and their composites were used as sensitizers in the fabricated DSSCs. The extracted dyes contain chlorophyll and anthocyanin color pigments. The characterisation techniques used in this study included FTIR which was used for determining chemical structural properties of the dye powders, UV-Visible spectroscopy was applied to determine the optical absorption properties of dye solutions, Raman spectroscopy and SEM were used for investigating crystalline structure and surface morphology of TiO_2 films respectively. TEM was also used to obtain the mean particle size of 12 ± 2 nm of TiO_2 particles. This study also presents DSSCs fabricated basing on individual dyes and their composites made from hibiscus flowers, pumpkin and sweet potato leaves. Table 5.1 shows the power conversion efficiencies obtained from the fabricated dye sensitized solar cells.

Table 5.1: Power conversion efficiencies of fabricated dye sensitized solar cells

Solar cell	PCE (%)
H	0.08
P	0.30
S	0.50
PH1:3	0.65
SH1:3	1.00

The results reveal that SH composite based DSSC at a ratio of 1:3 has the highest PCE of 1.0 % due to broader absorption in the visible region of the electromagnetic spectrum, high short circuit current and improved electron transfer to the semiconductor TiO_2 photoelectrode compared to single and PH dyes. The best performance exhibited by SH composite based DSSC shows that mixing of dyes from different plant materials could be a very attractive and effective technique for improving optical absorption properties and efficiency of natural dyes in DSSCs. The performance of dye sensitized solar cells (DSSCs) based on natural sensitizers reported in this study is generally low compared to commercial synthetic (organic) dyes, however, natural dyes are non toxic, cheap, involve easy preparation and compatible with

temperature changes. This is a motivation to probe efficient natural dye molecules as a replacement for commercial synthetic dyes that are toxic, expensive, environmentally non friendly and involve complicated preparation techniques. In addition, the highest efficiency obtained in this study can be used to power portable devices such as solar watches and solar calculators hence could solve some of the society challenges.

5.2 Recommendation

Further investigation should be carried out on the following work.

- Chemical structural and optical absorption properties of the dye extracts for DSSCs using methanol or any other solvent.
- Chemical structural and optical absorption properties of the extracted dyes for DSSCs keeping the mass of hibiscus dye constant and varying that of pumpkin and sweet potato dyes.
- Effect of concentration of the extracted dyes on DSSC performance.
- Effect of PH of dyes extracted from hibiscus flower, pumpkin and sweet potato leaves on the working of DSSCs.

REFERENCES

ABERLE, A. G. 2009. Thin-film solar cells. *Thin solid films,* 517**,** 4706-4710.

ABOU-RAS, D., KIRCHARTZ, T. & RAU, U. 2016. *Advanced characterization techniques for thin film solar cells*, John Wiley & Sons.

AKASH, M. S. H., REHMAN, K., AKASH, M. S. H. & REHMAN, K. 2020. Ultraviolet-visible (UV-VIS) spectroscopy. *Essentials of pharmaceutical analysis***,** 29-56.

ALIM, M. A., REPON, M. R., ISLAM, T., MISHFA, K. F., JALIL, M. A., ALJABRI, M. D. & RAHMAN, M. M. 2022. Mapping the Progress in Natural Dye-Sensitized Solar Cells: Materials, Parameters and Durability. *ChemistrySelect,* 7**,** e202201557.

BONACCORSO, F., SUN, Z., HASAN, T. & FERRARI, A. 2010. Graphene photonics and optoelectronics. *Nature photonics,* 4**,** 611-622.

BUTLER, K., FROST, J. & WALSH, A. 2015. Energy & Environ. Sci.

CALOGERO, G., BARTOLOTTA, A., DI MARCO, G., DI CARLO, A. & BONACCORSO, F. 2015. Vegetable-based dye-sensitized solar cells. *Chemical Society Reviews,* 44**,** 3244-3294.

CALOGERO, G. & DI MARCO, G. 2008. Red Sicilian orange and purple eggplant fruits as natural sensitizers for dye-sensitized solar cells. *Solar Energy Materials and Solar Cells,* 92**,** 1341-1346.

CHANG, H., KAO, M.-J., CHEN, T.-L., CHEN, C.-H., CHO, K.-C. & LAI, X.-R. 2013. Characterization of natural dye extracted from wormwood and purple cabbage for dye-sensitized solar cells. *International Journal of Photoenergy*, 2013.

CHO, K.-C., CHANG, H., CHEN, C.-H., KAO, M.-J. & LAI, X.-R. 2014. A study of mixed vegetable dyes with different extraction concentrations for use as a sensitizer for dye-sensitized solar cells. *International Journal of Photoenergy*, 2014.

CLEMENTSON, L. A. & WOJTASIEWICZ, B. 2019. Dataset on the absorption characteristics of extracted phytoplankton pigments. *Data in brief,* 24**,** 103875.

COMMITTEE, G. 2012. Tables for reference solar spectral irradiances: Direct normal and hemispherical on 37 tilted surface. *ASTM International*.

DESAI, N. D., KHOT, K. V., DONGALE, T., MUSSELMAN, K. P. & BHOSALE, P. N. 2019. Development of dye sensitized TiO2 thin films for efficient energy harvesting. *Journal of Alloys and Compounds*, 790**,** 1001-1013.

EVANS, L. 2004. UV-VIS Spectrophotometry: A Brief Background to Spectrophotometry. *Biochrom Ltd a division of harvad biosciencie, Inc***,** 1-15.

EZIKE, S. C., HYELNASINYI, C. N., SALAWU, M. A., WANSAH, J. F., OSSAI, A. N. & AGU, N. N. 2021. Synergestic effect of chlorophyll and anthocyanin Co-sensitizers in TiO2-based dye-sensitized solar cells. *Surfaces and Interfaces,* 22**,** 100882.

GORDON, R. G. 2000. Criteria for choosing transparent conductors. *MRS bulletin,* 25**,** 52-57.

GRANQVIST, C. G. 2007. Transparent conductors as solar energy materials: A panoramic review. *Solar energy materials and solar cells,* 91**,** 1529-1598.

GRÄTZEL, M. 2014. The light and shade of perovskite solar cells. *Nature materials,* 13**,** 838-842.

GREEN, M. A. 2005. Silicon photovoltaic modules: a brief history of the first 50 years. *Progress in Photovoltaics: Research and applications,* 13**,** 447-455.

GUPTA, S. K., DESAI, R., JHA, P. K., SAHOO, S. & KIRIN, D. 2010. Titanium dioxide synthesized using titanium chloride: size effect study using Raman spectroscopy and photoluminescence. *Journal of Raman Spectroscopy: An International Journal for Original Work in all Aspects of Raman Spectroscopy, Including Higher Order Processes, and also Brillouin and Rayleigh Scattering,* 41**,** 350-355.

HAMBERG, I. & GRANQVIST, C. G. 1986. Evaporated Sn-doped In2O3 films: Basic optical properties and applications to energy-efficient windows. *Journal of Applied Physics,* 60**,** R123-R160.

HAO, S., WU, J., HUANG, Y. & LIN, J. 2006. Natural dyes as photosensitizers for dye-sensitized solar cell. *Solar energy,* 80**,** 209-214.

HONSBERG, C. & BOWDEN, S. G. 2019. Photovoltaics education website. *PV Education*.

KALYANASUNDARAM, K. 2010. *Dye-sensitized solar cells*, CRC press.

KAY, A. & GRAETZEL, M. 1993. Artificial photosynthesis. 1. Photosensitization of titania solar cells with chlorophyll derivatives and related natural porphyrins. *The Journal of Physical Chemistry,* 97**,** 6272-6277.

KELLY, C. A. & MEYER, G. J. 2001. Excited state processes at sensitized nanocrystalline thin film semiconductor interfaces. *Coordination Chemistry Reviews,* 211**,** 295-315.

KIMPA, M. I., ISAH, K. U., YABAGI, J. A., TAUFIQ, S. & AGAM, M. A. B. 2017. Synthesis and characterization of natural sensitizers for dye sensitized solar cells. *Traektoriâ Nauki= Path of Science,* 3**,** 2001-2006.

KUCIAUSKAS, D., MONAT, J. E., VILLAHERMOSA, R., GRAY, H. B., LEWIS, N. S. & MCCUSKER, J. K. 2002. Transient absorption spectroscopy of ruthenium and osmium polypyridyl complexes adsorbed onto nanocrystalline TiO2 photoelectrodes. *The Journal of Physical Chemistry B,* 106**,** 9347-9358.

LAI, W. H., SU, Y. H., TEOH, L. G. & HON, M. H. 2008. Commercial and natural dyes as photosensitizers for a water-based dye-sensitized solar cell loaded with gold nanoparticles. *Journal of Photochemistry and Photobiology A: Chemistry,* 195**,** 307-313.

MACYK, W., SZACIŁOWSKI, K., STOCHEL, G., BUCHALSKA, M., KUNCEWICZ, J. & ŁABUZ, P. 2010. Titanium (IV) complexes as direct TiO2 photosensitizers. *Coordination Chemistry Reviews,* 254**,** 2687-2701.

MAURYA, I. C., GUPTA, A. K., SRIVASTAVA, P. & BAHADUR, L. 2016. Callindra haematocephata and Peltophorum pterocarpum flowers as natural sensitizers for TiO2 thin film based dye-sensitized solar cells. *Optical Materials,* 60**,** 270-276.

MEMMING, R. 1994. Photoinduced charge transfer processes at semiconductor electrodes and particles. *Electron Transfer I.* Springer.

MEYER, G. J. 1997. Efficient light-to-electrical energy conversion: nanocrystalline TiO2 films modified with inorganic sensitizers. ACS Publications.

MUNANDAR, M., HAKIM, A., PUSPITADINDHA, H., ANDIYANI, S. & NUROSYID, F. The effect of mixing Chlorophyll-Antocyanin as a natural source dye on the efficiency of dye-sensitized solar cell (DSSC). Journal of Physics: Conference Series, 2022. IOP Publishing, 012042.

NDEZE, U. I., AIDAN, J., EZIKE, S. C. & WANSAH, J. F. 2021. Comparative performances of nature-based dyes extracted from Baobab and Shea leaves photo-sensitizers for dye-sensitized solar cells (DSSCs). *Current Research in Green and Sustainable Chemistry,* 4**,** 100105.

OKTARIZA, L. G., YULIARTO, B. & SUYATMAN. Performance of dye sensitized solar cells (DSSC) using Syngonium Podophyllum Schott as natural dye and counter electrode. AIP Conference Proceedings, 2018. AIP Publishing LLC, 020022.

ONAH, E. O., OFFIAH, S., CHIME, U., WHYTE, G., OBODO, R. M., EKECHUKWU, O., AHMAD, I., UGWUOKE, P. & EZEMA, F. I. 2020. Comparative photo-response performances of dye sensitized solar cells using dyes from selected plants. *Surfaces and Interfaces*, 20**,** 100619.

OSSAI, A. N., EZIKE, S. C., TIMTERE, P. & AHMED, A. D. 2021. Enhanced photovoltaic performance of dye-sensitized solar cells-based Carica papaya leaf and black cherry fruit co-sensitizers. *Chemical Physics Impact*, 2**,** 100024.

PALUPI, E. K., NAZOPATUL, P., UMAM, R., ANDRIANA, B. B., SATO, H. & ALATAS, H. Molecular functional group and optical analysis on chlorophyll of green choy sum and cassava leaves extracts. IOP Conference Series: Earth and Environmental Science, 2020. IOP Publishing, 012030.

PANDIKUMAR, A., JOTHIVENKATACHALAM, K. & BHOJANAA, K. B. 2019. *Interfacial Engineering in Functional Materials for Dye-Sensitized Solar Cells*, John Wiley & Sons.

PARADIS, S., SIMANDL, G. & NEETZ, M. Indium, germanium and gallium in volcanic-and sediment-hosted base-metal sulphide deposits. Symposium on Strategic and Critical Materials Proceedings, November 13–14, 2015, Victoria, British Columbia, 2015. British Columbia Ministry of Energy and Mines, British Columbia Geological …, 23-29.

POLLY, S. J., BITTNER, Z. S., BENNETT, M. F., RAFFAELLE, R. P. & HUBBARD, S. M. Development of a multi-source solar simulator for spatial uniformity and close spectral matching to AM0 and AM1. 5. 2011 37th IEEE Photovoltaic Specialists Conference, 2011. IEEE, 001739-001743.

RAMKIRAN, B., SUNDARABALAN, C. & SUDHAKAR, K. 2020. Performance evaluation of solar PV module with filters in an outdoor environment. *Case Studies in Thermal Engineering*, 21**,** 100700.

REDDY, K. M., REDDY, C. G. & MANORAMA, S. 2001. Preparation, characterization, and spectral studies on nanocrystalline anatase TiO2. *Journal of Solid State Chemistry*, 158**,** 180-186.

ROSLI, N., SABANI, N., SHAHIMIN, M., JUHARI, N., SHAARI, S., AHMAD, M. & ZAKARIA, N. Dyes extracted from Hibiscus Sabdariffa flower and Pandannus amaryllifolius leaf as natural dye sensitizer by using an alcohol-based solvent. Journal of Physics: Conference Series, 2021. IOP Publishing, 012025.

SAHA, S., DAS, P., CHAKRABORTY, A. K., SARKAR, S. & DEBBARMA, R. 2016. Fabrication of DSSC with nanoporous TiO2 film and Kenaf Hibiscus dye as sensitizer. *International Journal of Renewable Energy Research (IJRER),* 6**,** 620-627.

SANJAY, P., DEEPA, K., MADHAVAN, J. & SENTHIL, S. 2018. Performance of TiO2 based dye-sensitized solar cells fabricated with dye extracted from leaves of Peltophorum pterocarpum and Acalypha amentacea as sensitizer. *Materials Letters,* 219**,** 158-162.

SINGH, E. & NALWA, H. S. 2015. Graphene-based dye-sensitized solar cells: a review. *Science of advanced Materials,* 7**,** 1863-1912.

SIRIMANNE, P. M., SENEVIRATHNA, M., PREMALAL, E. & PITIGALA, P. 2006. Enhancement of the photoproperties of solid-state TiO2| dye| CuI cells by coupling of two dyes. *Semiconductor science and technology,* 21**,** 818.

SUMIARNA, G. & MADDU, A. 2016. Dye-sensitized solar cell based on flower-like ZnO nanoparticles as photoanode and natural dye as photosensitizer.

VIEZBICKE, B. D., PATEL, S., DAVIS, B. E. & BIRNIE III, D. P. 2015. Evaluation of the Tauc method for optical absorption edge determination: ZnO thin films as a model system. *physica status solidi (b),* 252**,** 1700-1710.

WANG, W. & LAUMERT, B. 2014. Simulate a 'sun'for solar research: a literature review of solar simulator technology.

WEST, A. R. 2014. *Solid state chemistry and its applications*, John Wiley & Sons.

YOUNAS, M. & HARRABI, K. 2020. Performance enhancement of dye-sensitized solar cells via co-sensitization of ruthenium (II) based N749 dye and organic sensitizer RK1. *Solar Energy,* 203**,** 260-266.

YUNIATI, Y., ELIM, P., ALFANAAR, R. & KUSUMA, H. Extraction of anthocyanin pigment from hibiscus sabdariffa l. by ultrasonic-assisted extraction. IOP Conference Series: Materials Science and Engineering, 2021. IOP Publishing, 012032.

ZAINUL, R. & ISARA, L. Preparation of Dye Sensitized Solar Cell (DSSC) using anthocyanin color dyes from jengkol shell (Pithecellobium lobatum Benth.) by the gallate acid copigmentation. Journal of Physics: Conference Series, 2019. IOP Publishing, 012021.

ZULKIFILI, A. N. B., KENTO, T., DAIKI, M. & FUJIKI, A. 2015. The basic research on the dye-sensitized solar cells (DSSC). *Journal of Clean Energy Technologies*, 3**,** 382-387.

APPENDICES

APPENDIX A: Raw data

All the raw data is available with the Principal Investigator on request.

APPENDIX B: Publication from the dissertation

Mukhokosi, E.P., Maaza, M., Tibenkana, M., Botha, N.L., Namanya, L., Madiba, I.G. and Okullo, M., 2023. Optical absorption and photoluminescence properties of cucurbita maxima dye adsorption on TiO_2 nanoparticles. *Materials Research Express*.

APPENDIX C: Permission to reuse figures from other publications

Figures 2.1, 2.2, 2.3, 2.4, 2.5, 2.6, 2.7, 2.8, 2.11, 3.4 and 4.2 were reproduced with permission from the authors.

Materials Research Express

PAPER • OPEN ACCESS

Optical absorption and photoluminescence properties of Cucurbita maxima dye adsorption on TiO_2 nanoparticles

To cite this article: Emma Panzi Mukhokosi *et al* 2023 *Mater. Res. Express* **10** 046203

Materials Research Express

OPEN ACCESS

RECEIVED
18 January 2023

REVISED
17 March 2023

ACCEPTED FOR PUBLICATION
19 April 2023

PUBLISHED
27 April 2023

PAPER

Optical absorption and photoluminescence properties of Cucurbita maxima dye adsorption on TiO_2 nanoparticles

Emma Panzi Mukhokosi[1,*], Maliki Maaza[2,3], Muhammed Tibenkana[1], Nandipha L Botha[3], Loyce Namanya[1], I G Madiba[2,3] and Michael Okullo[1]

[1] Department of Physics, Faculty of Science, Kyambogo University, PO Box, 1, Kyambogo, Uganda
[2] College of Graduate Studies, UNESCO UNISA Africa Chair in Nanosciences & Nanotechnology, University of South Africa, Pretoria, South Africa
[3] Material Research Department, Nanosciences African Network (NANOAFNET), iThemba LABS, Cape Town, South Africa
* Author to whom any correspondence should be addressed.

E-mail: panzi2018@gmail.com

Keywords: DSSCs, Cucurbita maxima, TiO2, photoluminescence, adsorption

Abstract

Dye-sensitised solar cells (DSSCs) are 3rd generation photovoltaic device that imitate photosynthesis in plants. The fundamental concept of a DSSCs is that the photoanode is covered by the dye as a sensitiser. Natural dyes from plant-based extracts have gained attention as alternatives to toxic and expensive commercial dye sensitisers. Various studies have been conducted on the use of natural plant dye extracts for DSSCs . However, more fundamental studies on their adsorption on TiO_2 photoanode nanoparticles are still not well understood. In this study, we investigated the crystal structure, optical absorption, and photoluminescence properties of TiO_2, Cucurbita maxima, and Cucurbita maxima dyes adsorbed on TiO_2 nanoparticles as potential materials for DSSCs. Raman spectra confirmed the anatase phase of the TiO_2 nanoparticles. The particle size of 12 ± 2 nm was confirmed through the transmission electron microscope. The optical absorption properties of Cucurbita maxima show two distinct absorption bands: blue visible (450–500 nm) and red visible (635–674 nm). The photoluminescence spectra of the dye extract and its adsorption onto the TiO_2 nanoparticles showed two prominent peaks in the blue and red regions of the electromagnetic spectrum. No significant peak is observed in the green region of the electromagnetic spectrum. These studies shed more light on the fundamental properties of chlorophyll adsorption on TiO_2 nanoparticles and their optical and photoluminescence properties for applications as sensitisers in DSSCs.

1. Introduction

Dye-sensitised solar cells are 3rd generation solid-state photovoltaic devices that imitate photosynthesis in plants. The fundamental concept of DSSCs is that the photoanode is covered by the dye as a sensitiser. Dye-sensitised solar cells are preferred over other photovoltaics because they can be processed cheaply, and there is an abundance of materials that can be dispensed as portable devices and used in indoor facilities, such as chargers, solar keyboards, and solar bags [1]. The main components of DSSC are porous crystalline wide-semiconductor bandgap electrodes, dye sensitisers, electrolytes, and counter electrodes [2]. The sensitising dye is a crucial parameter, and the most efficient dyes are ruthenium (II) and osmium (II) complexes with interesting features such as good photon absorption in the visible range of the electromagnetic spectrum, with a long excited lifetime and high-efficiency metal-to-ligand charge transfer [3]. However, they are expensive, contain heavy metals which cause deleterious environmental effects, and require sophisticated preparation techniques [4]. Natural dye sensitisers are an attractive area of research because of the abundance, low cost, nontoxicity, and biodegradability of materials. Natural dye extracts from the leaves, roots, tree bark, and flowers have been studied and applied as sensitisers with acceptable levels of efficiency [5–10]. However, few experimental studies provide optical absorption and photoluminescence properties on the interaction of dye extracts with wide-

band-gap semiconductor materials; therefore, more fundamental studies on natural dye sensitisers are still needed. In this study, we investigated the optical and photoluminescence properties of Cucurbita maxima dye extract and its adsorption onto TiO_2 nanoparticles for potential applications in DSSCs. Raman spectra confirmed the anatase phase of the TiO_2 nanoparticles. The particle size of 12 ± 2 nm was confirmed through the transmission electron microscope. The optical absorption properties showed two distinct absorption bands in the blue visible (450–500 nm) and red visible (635–674 nm) regions of the electromagnetic spectrum. The photoluminescence spectra of the dye extract and its adsorption onto the TiO_2 nanoparticles showed two peaks in the blue and red regions of the electromagnetic spectrum with no green luminescence. These studies shed light on the fundamental properties of chlorophyll adsorption on TiO_2 nanoparticles and their optical and photoluminescence properties for applications as sensitisers in photovoltaic devices such as DSSCs.

2. Materials and methods

TiO_2 powder with a particle size < 25 nm (anatase phase) obtained from Sigma Aldrich was used for the preparation of TiO_2 thin films. The soda-lime glass substrate (SLG) was cleaned thoroughly using deionised (DI) water followed by ethanol. The mixture was sonicated for 3 h in a mixture of DI water and ethanol. One gram of TiO_2 nano-powder was dissolved in 300 mg of polyethylene glycol containing a mixture of 6 ml of glacial acetic acid and 6 ml of double-distilled water. The mixture was placed in an ultrasonic bath for three hours. Then, 200 μl was drop-casted on a soda lime glass substrate twice and left to dry at room temperature (30 °C). The thin films were annealed at 450 °C for 30 min in a tubular furnace in air. The furnace was naturally cooled to room temperature. The annealed TiO_2 nanoparticles on SLG were soaked in the dye for 24 h and then removed and kept in the dark at room temperature for 30 days before further characterisation.

2.1. Chlorophyll extraction and adsorption

Pumpkin (Cucurbita maxima) leaves were collected from Ugandan flora and washed with tap water, followed by distilled water, and dried in an oven for 24 h at 60 °C. The dried leaves were pounded into a powder form using a mortar and pestle. Pumpkin leaf powder (10 g) was dissolved in 20 ml of ethanol in amber bottles placed in the dark for 36 h. The dye was then filtered through Whatman filter paper number 3 and stored in amber bottles for further investigation.

2.2. Characterization methods

The structural properties of the TiO_2 thin films were investigated using Raman spectroscopy with a 532 nm laser. The optical absorption properties of the TiO_2 thin films and pumpkin dye extracts were investigated using a UV–visible–NIR spectrophotometre in the 200–1100 nm range. The photoluminescence (PL) properties of the TiO_2 thin films, pumpkin leaf powder, and pumpkin dye adsorption on TiO_2 nanoparticles were investigated using an FL spectrometer instrument with a 350-nm laser source. High-resolution transmission electron microscopy (HRTEM) with an accelerating voltage of 200 kV was used to investigate the size of the TiO_2 nanoparticles. Scanning electron microscopy (SEM) was used to investigate the surface morphology of TiO_2 nanoparticles. The elemental composition of the TiO_2 nanoparticles was investigated using energy-dispersive x-ray spectroscopy (EDX). The details of the SEM, TEM, PL, and UV–vis-NIR instruments were the same as those reported elsewhere [11].

3. Results and discussion

3.1. Structural and surface morphology

The Raman spectra of the pristine and dye-sensitised TiO_2 nanoparticles are shown in figure 1(a). The spectra show vibrational bands at 141 (E_g), 193 (E_g), 393 (B_{1g}), 514 (B_{1g}), and 636 (E_g) cm^{-1}, which are characteristics of the TiO_2 anatase phase of space group $I4_1/amd$ [12–14]. It is noted that the Raman spectra of dye-sensitised TiO_2 nanoparticles have broader and more intense peaks than those of pristine one, which could be attributed to the reduction in defect states when the dye was adsorbed onto the TiO_2 nanoparticles. The surface morphologies of the pristine and dye-sensitised TiO_2 nanoparticles are shown in figures 1(b) and (c), respectively. The surface consists of agglomerated, rough, and nano-sized randomly distributed particles for the pristine TiO_2 nanoparticles, which is advantageous for dye adsorption. For dye-sensitised TiO_2 nanoparticles, fairly uniform, well-connected, and distributed nanoparticles are observed, which may result in improved photon-to-electric conversion efficiency [15]. The EDX spectra of the pristine and sensitised TiO_2 nanoparticles are shown in the insets of figures 1(b) and (c), respectively. The average elemental composition shows the presence of Ti (~ 56.6%), O (~ 43.4%) for pristine and O (~ 61.2%), Ti (~ 31.8%) for dye-sensitized TiO_2 nanoparticles. This elemental composition is within the expected stoichiometry. The slight change in the elemental concentration is

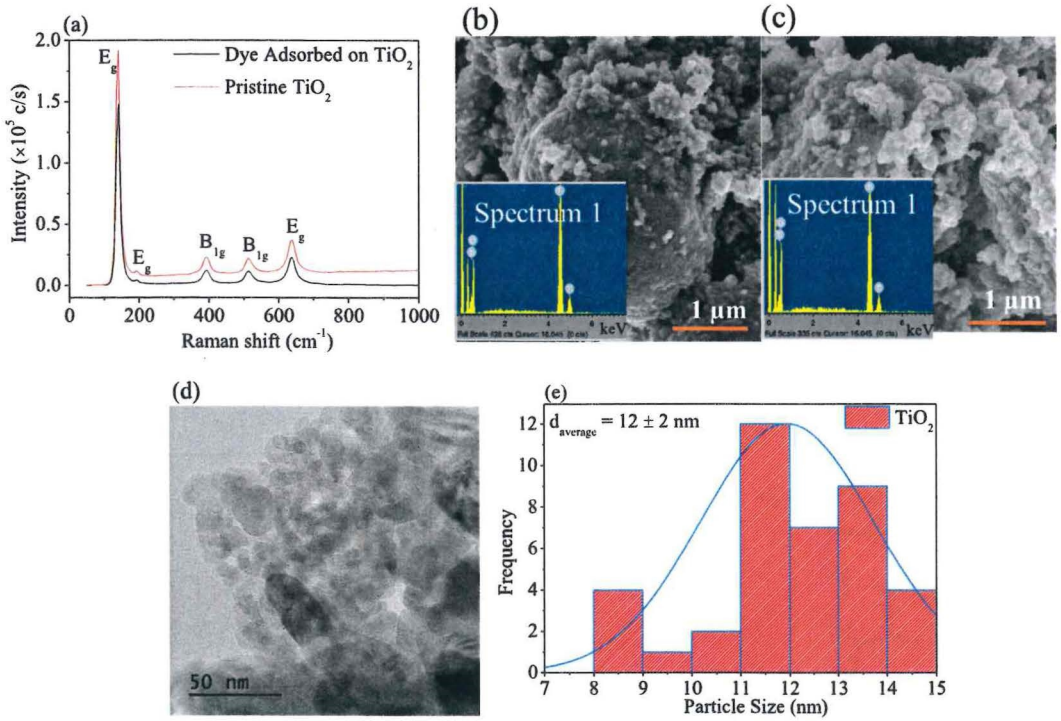

Figure 1. (a) Raman spectra of pristine and dye sensitized TiO_2 nanoparticles, (b) Surface morphology of pristine TiO_2 nanoparticle, (c) Surface morphology of dye-sensitized TiO_2 nanoparticles, (d) TEM image of pristine TiO_2 nanoparticles, (e) Bar graph showing pristine TiO_2 particle size distribution. The inset in figure b is EDX spectra of pristine TiO_2 nanoparticle and the inset in figure c is EDX spectra of dye-sensitized TiO_2 nanoparticles.

attributed to the change in the bond length in TiO_2 owing to the adsorption of the dye on the TiO_2 nanoparticles [15]. The TEM image shown in figure 1(d) confirms that the TiO_2 nanoparticles with a normal distribution were fitted using ImageJ software [16]. The TiO_2 nanoparticles showed a normal distribution, with a mean particle size of 12 ± 2 nm, as shown in figure 1(e).

3.2. Optical properties of pumpkin dye extracts

The optical absorption properties of Cucurbita maxima leaf dye extract at different concentrations are shown in figure 2(a). Five broad absorption bands were observed in the ranges of <400, 450–500, 521–551, 596–630, and 635–674 nm for all concentrations, with maximum peaks located at 333, 421, 462, 533, 613, and 662 nm, respectively, as shown in figures 2(a) and (b) respectively. A peak at approximately 333 nm represents the existence of C=O or C=C functional groups that are responsible for the n–π^* electronic transition that can initiate electrical circuits in DSSCs and can facilitate their adsorption onto TiO_2 surfaces [17, 18]. Two prominent absorption bands in the blue visible (450–500 nm) and red visible (635–674 nm) ranges have been observed in other related studies and are attributed to the presence of chlorophyll b and chlorophyll a [19, 20]. From figure 1(a), it is observed that the absorbance increases with dye concentration and can follow the Beer–Lambert Law represented by equation (1).

$$A = \varepsilon Cl \tag{1}$$

Where A absorbance, ε is the molar absorption coefficient, C is the molar concentration, and l is the optical path length [21]. Broadening of the bands in the range 635–674 nm was observed for higher concentrations, indicating chlorophyll-chlorophyll interactions, as has been observed in similar studies [19]. The bandgap energy of the material in the solid-state form is the difference between the conduction and valence band energies. In organic molecules, the valence band is represented by the highest occupied molecular orbitals (HOMOs), and the conduction band is represented by the lowest unoccupied molecular orbitals (LUMOs) [22]. The value of the band gap for organic dyes can easily be obtained from the maximum absorption peak in the UV-Visible spectra and computed using the relation

$$E = \frac{h\nu}{\lambda_{max}} = \frac{1240}{\lambda_{max}}(eV) \tag{2}$$

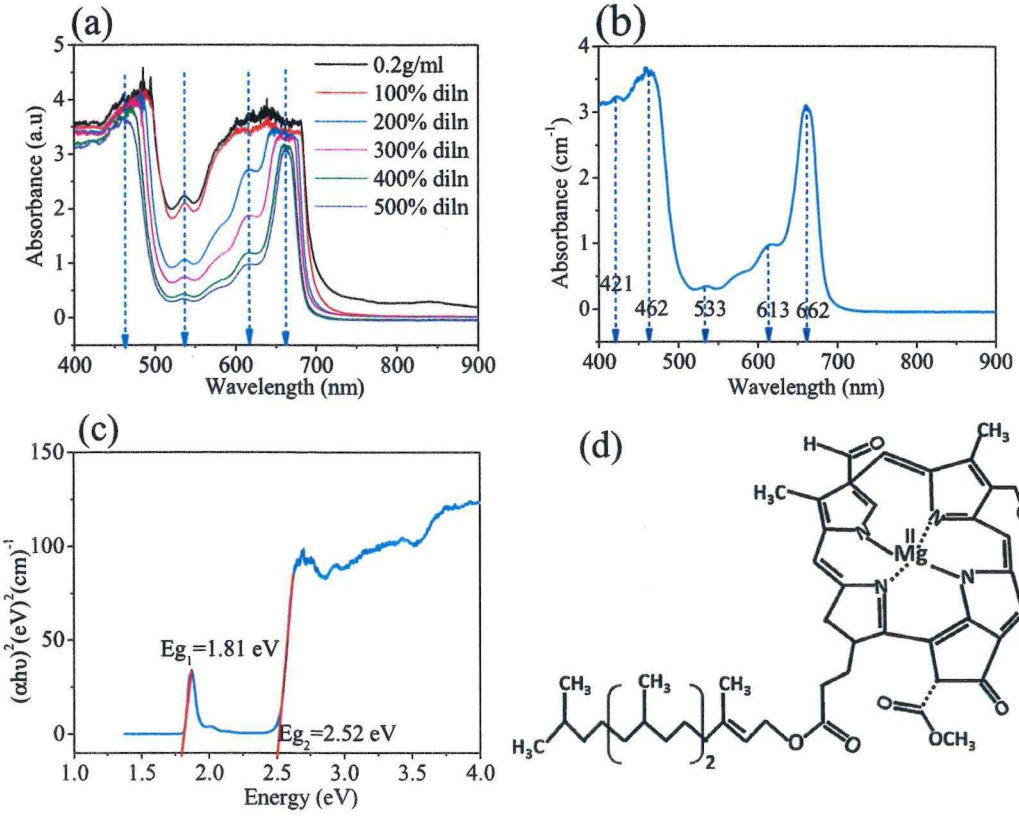

Figure 2. (a) Absorbance versus wavelength of pumpkin dye extract at different concentrations, (b) Isolated spectra without saturation for peak identification, (c) Tauc plot for direct band transitions of the dye extract and (d) General chemical structure of Chlorophyll. Reprinted from [30], © 2018 Elsevier GmbH. All rights reserved.

where λ_{max} is the maximum wavelength in the absorption spectrum. The calculated band gap using this approach were 3.72, 2.95, 2.68, 2.33, 2.02, and 1.87 eV for λ_{max} corresponding to absorption peaks located at wavelengths of 333, 421, 462, 533, 613, and 662 nm respectively. To ascertain the accuracy of these energy values, the band gap of the Cucurbita maxima dye extract was estimated using the Tauc plot, as shown in figure 2(c) for direct optical transitions. The Tauc plots were based on equation (3).

$$(\alpha h\upsilon)^n = A(h\upsilon - E_g) \tag{3}$$

where α is the material-dependent absorption coefficient, $h\upsilon$ is the photon energy, A is a constant, E_g is the optical bandgap, and n is the type of electronic transition, which is 2 for the direct band gap and ½ for the indirect band gap [23–26]. The direct allowed band gaps were calculated as 1.81 and 2.52 eV. These two band gaps are consistent with the energies corresponding to the maximum absorption peaks at 662 (1.87 eV) and 462 nm (2.68 eV), respectively. These energies represent two optical windows for light absorption by the chlorophyll. Blue visible region and near-red visible region of the electromagnetic spectrum. The values of the bandgap in the two optical absorption windows in the visible range show that the extracted dye can be an effective sensitiser for photovoltaic applications. The Tauc plot method is known to provide approximate values of the band gap because it assumes an ideal parabolic band structure and depends on the type of transition [27]. This method has been adopted to calculate the band gap for chlorophyll a and anthocyanin pigments in related studies with acceptable levels of accuracy [17, 19, 20, 28, 29]. The general molecular structure of chlorophyll is shown in figure 2(d).

3.3. Optical absorption properties of TiO_2

3.3.1. Thin film and TiO_2/Dye adsorption

We investigated the optical properties of nanocrystalline TiO_2 thin films on soda-lime glass substrate (SLG) and Cucurbita maxima dye adsorption on TiO_2 nanoparticles using diffuse reflectance spectra (DRS), as shown in figure 3(a). The DRS was then converted to an equivalent absorption spectrum using the Kubelka-Munk (KM) function described in detail elsewhere [24, 33]. This function is represented by equation (4).

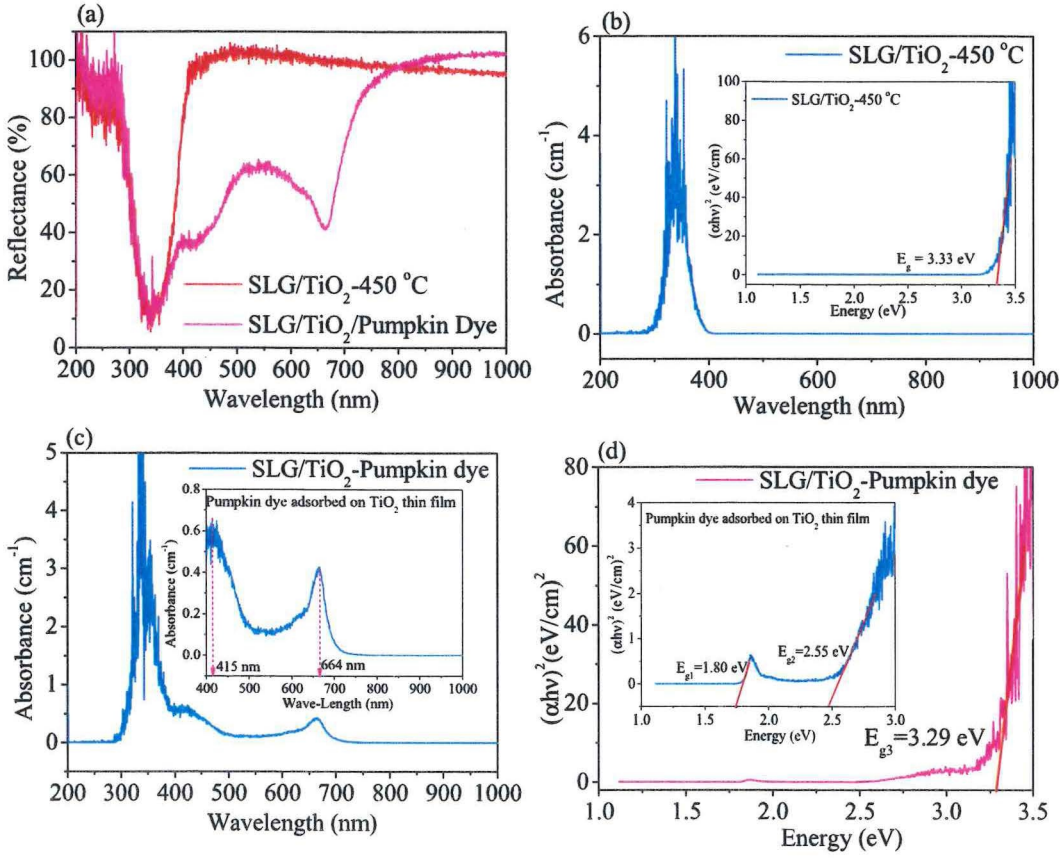

Figure 3. (a) Diffuse reflection spectra (DRS) of TiO_2 on soda lime glass substrate (SLG) and pumpkin dye adsorption on TiO_2, (b) absorbance versus wavelength and in-set is Tauc plot for TiO_2 thin film on SLG, (c) Absorbance versus wavelength and in-set is magnified image for the region of pumpkin dye adsorption on TiO_2 thin film, (d) Tauc plot for SLG/TiO_2-pumpkin dye adsorption and in-set is magnified image for the region of pumpkin dye adsorption on TiO_2 thin film. Experiments on SLG/TiO_2/Pumpkin dye adsorption were carried out after 30 days.

$$F(R) = \frac{(1-R)^2}{2R} \tag{4}$$

These terms have their usual meaning, as described elsewhere [24]. The band gap was computed by making a Tauc plot related to equation (5)

$$(F(R)h\upsilon) = A(h\upsilon - E_g)^n \tag{5}$$

The terms in equation (5) have their usual meanings, as explained in previous related studies [11, 34]. The optical bandgap of the TiO_2 sample was estimated from the Tauc plot, as shown in the inset of figure 3(b), that is, a plot of $(\alpha h\nu)^2$ against $h\nu$ for the direct bandgap material and calculated from the linear fit as 3.33 eV. The absorbance of Cucurbita adsorbed on TiO_2 nanoparticles is shown in figure 3(c), which shows three distinct regions, which correspond to the optical bands for TiO_2 in the Uv region: Cucurbita maxima in the blue visible (450–500 nm) and red visible (635–674 nm) ranges which imply the presence of chlorophyll b and chlorophyll a, respectively, that have been adsorbed on the TiO_2 nanoparticles [19, 20]. The inset of figure 3(c) shows the enlarged region of the expected region where the adsorption of Cucurbita maxima dye on TiO_2 nanoparticles is expected. The bandgap was estimated using a Tauc plot, as shown in figure 3(d). The inset of figure 3(d) shows an enlarged region of Cucurbita maxima dye adsorption. Three band gaps were estimated as 3.29 eV corresponding to TiO_2 region, 1.88 and 2.55 eV corresponding to the absorption region of Cucurbita maxima adsorbed on TiO_2 nanoparticles. These studies confirm that Cucurbita maxima can be used as an effective sensitiser for applications in DSSCs.

3.3.2. Photoluminescence properties of TiO_2 thin film and TiO_2-Pumpkin dye adsorption

Photoluminescence of dye pigments is important for establishing a link between photoemission and the conversion to photoelectricity from natural plant-based dye sensitisers for DSSCs applications [35]. Figures 4(a)–(c) show the photoluminescence emission spectra of TiO_2 nanoparticles, Cucurbita maxima powder dye, and Cucurbita maxima dye adsorption on TiO_2 nanoparticles, respectively. For the TiO_2 nanoparticles, it was found

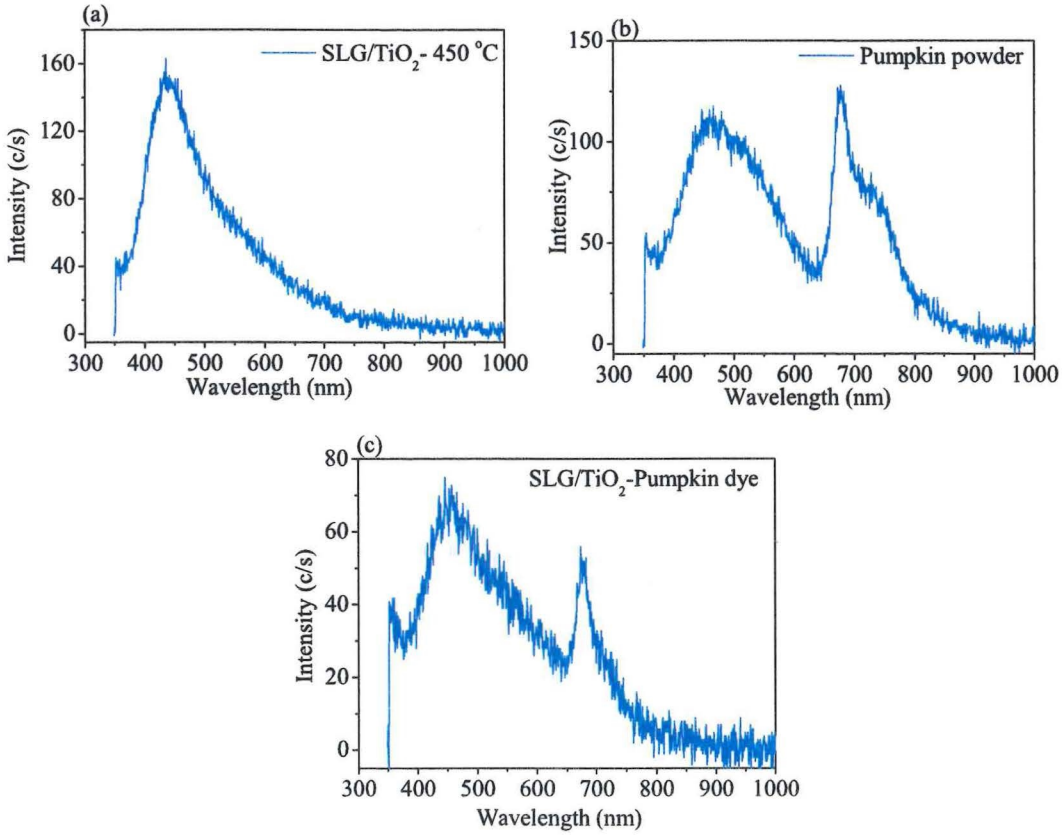

Figure 4. (a) PL spectra of TiO_2 on SLG annealed at 450 °C, (b) PL spectra of pumpkin powder and (c) PL spectra of SLG/TiO_2-pumpkin dye adsorption after 30 days.

that the maximum peak intensity was approximately 435 nm. Three peaks were observed for C. maxima. A broad peak was observed in the blue region with a maximum intensity of 462 nm, a sharp peak at 675 nm in the red region, and an arm at approximately 726 nm. These peak intensities correspond to energy values of 2.85 eV for TiO_2 and 2.68, 1.83, and 1.71 eV for Cucurbita maxima. Two peaks were identified for the Cucurbita dye extract adsorbed on TiO_2 nanoparticles, two peaks are identified. They are positioned in the blue region at 451 nm, corresponding to 2.75 eV, and red region at 677 nm to 1.83 eV. The energy values were consistent with those obtained by UV–vis spectroscopy. No green emission intensity is observed in the spectra. Similar peaks were observed in other studies [36]. Figure 4(c) shows that the photoluminescence peak at 726 nm disappeared. The disappearance of this photoluminescence peak may improve the optoelectronic performance of the solar cells [37–39].

4. Conclusion and way forward

We provided the crystal structural, optical, and photoluminescence properties of TiO_2, Cucurbita maxima, and Cucurbita maxima dye adsorbed on TiO_2 nanoparticles for potential application in DSSCs. The optical absorption properties of Cucurbita maxima show two prominent absorption bands: blue visible (450–500 nm) and red visible (635–674 nm). The photoluminescence spectra of the dye extract and its adsorption on the TiO_2 nanoparticles showed two prominent peaks in the blue and red regions of the electromagnetic spectrum, and no significant peak was observed in the green region of the electromagnetic spectrum. This study provides a more fundamental understanding of the applications of chlorophyll as a sensitiser in DSSCs. For future applications in DSSCs, and for effective optical absorption across the entire UV–visible–near-infrared range electromagnetic spectrum, it is recommended to make a composite of Cucurbita maxima dye extract with another pigment that absorbs in the green region to enhance the photo-absorption and improve the photo-to-electric conversion efficiency in DSSCs.

Acknowledgments

This research was financially supported by The World Academy of Sciences-United Nations Educational, Scientific and Cultural Organisation (TWAS-UNESCO) Associateship Scheme at the Centres of Excellence in the South fellowship program, the United Nations Educational, Scientific and Cultural Organisation-University of South Africa (UNESCO-UNISA) Africa Chair in Nanosciences & Nanotechnology, the Nano-sciences African Network (NANOAFNET) and Kyambogo University Competitive Research Grants. We appreciate Juma Moses Wabwile of Physics Department of University of Nairobi for carrying out the Raman Spectra Experiment. We would like to thank Editage (www.editage.com) for English language editing.

Data availability statement

All data that support the findings of this study are included within the article (and any supplementary files).

Author contributions

All authors contributed to the study conception and design. Material preparation, data collection and analysis were performed by Emma Panzi Mukhokosi and Maliki Maaza. The first draft of the manuscript was written by Emma Panzi Mukhokosi. All authors read and approved the final manuscript.

Conflict of interest

The authors declare that there is no conflict of interest regarding the publication of this article.

Supplementary information

Not applicable.

Ethical approval

Not applicable.

ORCID iDs

Emma Panzi Mukhokosi https://orcid.org/0000-0001-9229-3821

References

[1] Gong J, Sumathy K, Qiao Q and Zhou Z 2017 Review on dye-sensitized solar cells (DSSCs): Advanced techniques and research trends *Renew. Sustain. Energy Rev.* **68** 234–46
[2] Sharma K, Sharma V and Sharma S S 2018 Dye-Sensitized solar cells: fundamentals and current status *Nanoscale Res. Lett.* **13** 1–46
[3] Mozaffari S A, Saeidi M and Rahmanian R 2015 Photoelectric characterization of fabricated dye-sensitized solar cell using dye extracted from red Siahkooti fruit as natural sensitizer *Spectrochim. Acta - Part A Mol. Biomol. Spectrosc.* **142** 226–31
[4] Singh E and Nalwa H S 2015 Graphene-based dye-sensitized solar cells: a review *Sci. Adv. Mater.* **7** 1863–912
[5] Chandra Maurya I, Singh S, Srivastava P, Maiti B and Bahadur L 2019 Natural dye extract from Cassia fistula and its application in dye-sensitized solar cell: experimental and density functional theory studies *Opt. Mater. (Amst).* **90** 273–80
[6] Kumavat P P, Sonar P and Dalal D S 2017 An overview on basics of organic and dye sensitized solar cells, their mechanism and recent improvements *Renew. Sustain. Energy Rev.* **78** 1262–87
[7] Gu P, Yang D, Zhu X, Sun H and Li J 2018 Fabrication and characterization of dye-sensitized solar cells based on natural plants *Chem. Phys. Lett.* **693** 16–22
[8] Al-Alwani M A M, Mohamad A B, Ludin N A, Kadhum A A H and Sopian K 2016 Dye-sensitised solar cells: development, structure, operation principles, electron kinetics, characterisation, synthesis materials and natural photosensitisers *Renew. Sustain. Energy Rev.* **65** 183–213
[9] Anoua R, Touhtouh S, El Jouad M, Hajjaji A, Bakasse M, Sahraoui B, Płóciennik P and Zawadzka A 2022 Absorbance and photoluminescence study of pomegranate for dye-sensitized solar cells *Mater. Today Proc.* **66** 109–11
[10] Yadav S C, Tiwari M K, Kanwade A, Lee H, Ogura A and Shirage P M 2023 Butea monosperma, crown of thorns, red lantana camara and royal poinciana flowers extract as natural dyes for dye sensitized solar cells with improved efficiency *Electrochim. Acta* **441** 141793
[11] Aldeen T S, Ahmed Mohamed H E and Maaza M 2022 ZnO nanoparticles prepared via a green synthesis approach: physical properties, photocatalytic and antibacterial activity *J. Phys. Chem. Solids* **160** 110313

[12] Medjaldi F, Bouabellou A, Bouachiba Y, Taabouche A, Bouatia K and Serrar H 2020 Study of TiO2 , SnO2 and nanocomposites TiO2 : SnO2 thin films prepared by sol-gel method : Successful elaboration of variable—refractive index systems *Mater. Res. Express* **7** 016439
[13] Apopei P, Catrinescu C, Teodosiu C and Royer S 2014 Mixed-phase TiO2 photocatalysts: crystalline phase isolation and reconstruction, characterization and photocatalytic activity in the oxidation of 4-chlorophenol from aqueous effluents *Appl. Catal. B Environ.* **160–161** 374–82
[14] Choi H C, Jung Y M and Kim S B 2005 Size effects in the Raman spectra of TiO2 nanoparticles *Vib. Spectrosc.* **37** 33–8
[15] Ananth S, Vivek P, Saravana Kumar G and Murugakoothan P 2015 Performance of Caesalpinia sappan heartwood extract as photo sensitizer for dye sensitized solar cells *Spectrochim. Acta - Part A Mol. Biomol. Spectrosc.* **137** 345–50
[16] Abràmoff M D, Magalhães P J and Ram S J 2004 Image processing with imageJ *Biophotonics Int.* **11** 36–41
[17] Alhorani S, Kumar S, Genwa M and Meena P L 2021 Dye extracted from Bael leaves as a photosensitizer in dye sensitized solar cell *Mater. Res. Express* **8** 115507
[18] Zhang L and Cole J M 2015 Anchoring groups for dye-sensitized solar cells *ACS Appl. Mater. Interfaces* **7** 3427–55
[19] Alhorani S, Kumar S, Genwa M and Meena P L 2022 Performance of dye-sensitized solar cells extracted dye from wood apple leaves *J. Phys. Commun.* **6** 085012
[20] Milenković S M, Zvezdanović J B, Andelković T D and Marković D Z 2012 The identification of chlorophyll and its derivatives in the pigment mixtures: HPLC-chromatography, visible and mass spectroscopy studies *Adv. Technol.* **1** 16–24
[21] Yu Q *et al* 2022 Liquid-liquid phase reaction between crystal violet and sodium hydroxide: kinetic study and precipitate analysis *R. Soc. Open Sci.* **9** 220494
[22] Travaly Y, Bertrand P, Rignanese G M and Gonze X 1998 Theoretical modeling of the nucleation and growth of aluminium films thermally evaporated onto Poly(ethylene terephthalate) substrate *J. Adhes.* **66** 339–55
[23] Saikumari N, Preethi T, Abarna B and Rajarajeswari G R 2019 Ecofriendly, green tea extract directed sol–gel synthesis of nano titania for photocatalytic application *J. Mater. Sci., Mater. Electron.* **0** 0
[24] Mukhokosi E P, Krupanidhi S B and Nanda K K 2017 Band gap engineering of hexagonal SnSe2 nanostructured thin films for infra-red photodetection *Sci. Rep.* **7** 15215
[25] Mukhokosi E P, Krupanidhi S B and Nanda K K 2018 An extrinsic approach toward achieving fast response and self-powered photodetector *Phys. Status Solidi Appl. Mater. Sci.* **215** 1800470
[26] Mukhokosi E P, Roul B, Krupanidhi S B and Nanda K K 2019 Toward a fast and highly responsive SnSe 2 -based photodiode by exploiting the mobility of the counter semiconductor *ACS Appl. Mater. Interfaces* **11** 6184–94
[27] Segura A, Sánchez-Royo J F, García-Domene B and Almonacid G 2011 Current underestimation of the optical gap and Burstein-Moss shift in CdO thin films: a consequence of extended misuse of α^2-versus-hν plots *Appl. Phys. Lett.* **99** 2–5
[28] Mahadik S A, Yadav H M and Mahadik S S 2022 Surface properties of chlorophyll-a sensitized TiO2 nanorods for dye-sensitized solar cells applications *Colloids Interface Sci. Commun.* **46** 100558
[29] dos Santos F M M, Leite A M B, da Conceição L R B, Sasikumar Y, Atchudan R, Pinto M F, Suresh Babu R and de Barros A L F 2022 Effect of bandgap energies by various color petals of Gerbera jamesonii flower dyes as a photosensitizer on enhancing the efficiency of dye-sensitized solar cells *J. Mater. Sci., Mater. Electron.* **33** 20338–52
[30] Adedokun O, Sanusi Y K and Awodugba A O 2018 Solvent dependent natural dye extraction and its sensitization effect for dye sensitized solar cells *Optik (Stuttg).* **174** 497–507
[31] Ezike S C, Hyelnasinyi C N, Salawu M A, Wansah J F, Ossai A N and Agu N N 2021 Synergestic effect of chlorophyll and anthocyanin Co-sensitizers in TiO2-based dye-sensitized solar cells *Surfaces and Interfaces* **22** 100882
[32] Israsena Na Ayudhya T, Posey F T, Tyus J C and Dingra N N 2015 Using a microscale approach to rapidly separate and characterize three photosynthetic pigment species from fern *J. Chem. Educ.* **92** 920–3
[33] Vesna Džimbeg-Malčić Željka Barbarić-Mikočević K I 2011 Kubelka-Munk theory in describing optical properties of paper (I) *Teh. Vjesn.* **18** 117–24
[34] Chand P, Gaur A and Kumar A 2013 Structural, optical and ferroelectric behavior of hydrothermally grown ZnO nanostructures *Superlattices Microstruct.* **64** 331–42
[35] Shobana M, Balraju P, Senthil Kumar P, Muthukumarasamy N, Yuvakkumar R and Velauthapillai D 2022 Investigation on the performance of nanostructure TiO2 bi-layer as photoanode for dye sensitized solar cell application *Sustain. Energy Technol. Assessments* **52** 102295
[36] Adedokun O, Adedeji O L, Bello I T, Awodele M K and Awodugba A O 2021 Fruit peels pigment extracts as a photosensitizer in ZnO-based Dye-Sensitized solar cells *Chem. Phys. Impact* **3** 100039
[37] Lin Y, Lin G, Sun B and Guo X 2018 Nanocrystalline perovskite hybrid photodetectors with high performance in almost every figure of merit *Adv. Funct. Mater.* **28** 1705589
[38] Wu W S, Hao H L, Zhang Y X, Li J, Wang J J and Shen W Z 2018 Correlation between luminescence and structural evolution of colloidal silicon nanocrystals synthesized under different laser fl uences *Nanotechnology* **29** 025709
[39] Hao H L, Wu W S, Zhang Y, Wu L K and Shen W Z 2016 Origin of blue photoluminescence from colloidal silicon nanocrystals fabricated by femtosecond laser ablation in solution *Nanotechnology* **27** 325702

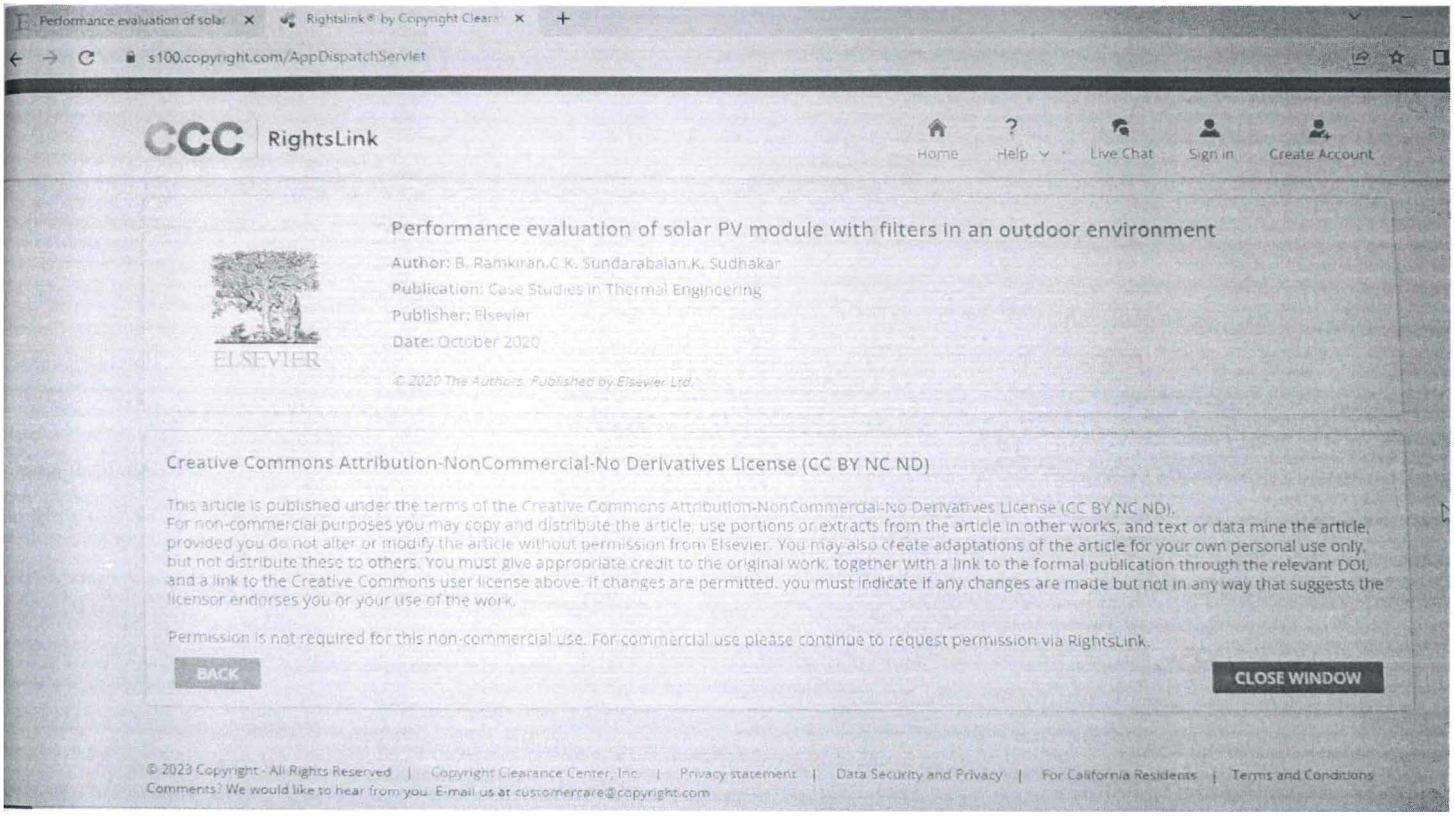

Chemical Society reviews

Publication type: Journal
Article: Vegetable-based dye-sensitized solar cells.

ISSN: 0306-0012
Publication Year: 1972 - Present
Publisher: ROYAL SOCIETY OF CHEMISTRY, ETC.)
Language: English
Country: United Kingdom of Great Britain and Northern Ireland
Rightsholder: Royal Society of Chemistry

View all details

Request Details | Additional Details

ADDITIONAL DETAILS

Order Reference Number	https://doi.org/10.1039/C4CS00309H	Additional information for your request	
The Requesting Person/Organization to Appear on the License	Tibenkana Mohammad	Attachment	Attach File — No file attached (.pdf, .jpg, .gif, .tiff, .png)

REQUESTED CONTENT DETAILS

Title, Description or Numeric Reference of the Portion(s)	Vegetable-based dye-sensitized solar cells	Title of the Article/Chapter the Portion is From	Vegetable-based dye-sensitized solar cells.
Editor of Portion(s)	Calogero, Giuseppe; Bartolotta, Antonino; Di M	Author of Portion(s)	Calogero, Giuseppe; Bartolotta, Antonino; Di M
Volume / Edition	44	Issue, if Republishing an Article From a Serial	10
Page or Page Range of Portion	3244-3294	Publication Date of Portion	2015-05-21

WILEY

Book: Solid State Chemistry and its Applications, 2nd Edition, Student Edition
Author: Anthony R. West
Publisher: John Wiley and Sons
Date: Mar 1, 2014

Order Completed

Thank you for your order.

This Agreement between Mr. Mohammad Tibenkana ("You") and John Wiley and Sons ("John Wiley and Sons") consists of your license details and the terms and conditions provided by John Wiley and Sons and Copyright Clearance Center.

Your confirmation email will contain your order number for future reference.

Printable Details

License Number	5553820575959
License date	May 21, 2023

Licensed Content

Licensed Content Publisher	John Wiley and Sons
Licensed Content Publication	Wiley Books
Licensed Content Title	Solid State Chemistry and its Applications, 2nd Edition, Student Edition
Licensed Content Author	Anthony R. West
Licensed Content Date	Mar 1, 2014
Licensed Content Pages	1

Order Details

Type of use	Dissertation/Thesis
Requestor type	University/Academic
Format	Electronic
Portion	Figure/table
Number of figures/tables	3
Will you be translating?	No

About Your Work

Title	CHEMICAL STRUCTURAL AND OPTICAL ABSORPTION PROPERTIES OF DYES EXTRACTED FROM SELECTED PLANT MATERIALS FOR DYE SENSITIZED SOLAR CELLS
Institution name	Kyambogo University
Expected presentation date	May 2023

Additional Data

Order reference number	9781119942948
Portions	6.19a, 6.9, 6.5

Requestor Location

Requestor Location	Mr. Mohammad Tibenkana Kyambogo Kampala, Central 0000 Uganda Attn: Mr. Mohammad Tibenkana

Tax Details

Publisher Tax ID	EU826007151

Price

Total	0.00 USD

Total: 0.00 USD

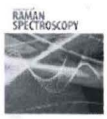

Titanium dioxide synthesized using titanium chloride: size effect study using Raman spectroscopy and photoluminescence

Author: D. Kirin, Satyaprakash Sahoo, Prafulla K. Jha, et al
Publication: Journal of Raman Spectroscopy
Publisher: John Wiley and Sons
Date: Sep 15, 2009

Order Completed

Thank you for your order.

This Agreement between Mr. Mohammad Tibenkana ("You") and John Wiley and Sons ("John Wiley and Sons") consists of your license details and the terms and conditions provided by John Wiley and Sons and Copyright Clearance Center.

Your confirmation email will contain your order number for future reference.

License Number	5551820723552
License date	May 18, 2023

Printable Details

Licensed Content

Licensed Content Publisher	John Wiley and Sons
Licensed Content Publication	Journal of Raman Spectroscopy
Licensed Content Title	Titanium dioxide synthesized using titanium chloride: size effect study using Raman spectroscopy and photoluminescence
Licensed Content Author	D. Kirin, Satyaprakash Sahoo, Prafulla K. Jha, et al
Licensed Content Date	Sep 15, 2009
Licensed Content Volume	41
Licensed Content Issue	3
Licensed Content Pages	6

Order Details

Type of use	Dissertation/Thesis
Requestor type	University/Academic
Format	Electronic
Portion	Figure/table
Number of figures/tables	1
Will you be translating?	No

About Your Work

Title	CHEMICAL STRUCTURAL AND OPTICAL ABSORPTION PROPERTIES OF DYES EXTRACTED FROM SELECTED PLANT MATERIALS FOR DYE SENSITIZED SOLAR CELLS
Institution name	Kyambogo University
Expected presentation date	May 2023

Additional Data

Order reference number	https://doi.org/10.1002/jrs.2427
Portions	Figure 3

Requestor Location

Requestor Location	Mr. Mohammad Tibenkana Kyambogo Kampala, Central 0000 Uganda Attn: Mr. Mohammad Tibenkana

Tax Details

Publisher Tax ID	EU826007151

Price

Total	0.00 USD

WILEY

Book: Advanced Characterization Techniques for Thin Film Solar Cells
Chapter: Absorption and Photocurrent Spectroscopy with High Dynamic Range
Author: Thomas Kirchartz, Thomas Christian Mathias Müller
Publisher: John Wiley and Sons
Date: Jul 22, 2016

Order Completed

Thank you for your order.

This Agreement between Mr. Mohammad Tibenkana ("You") and John Wiley and Sons ("John Wiley and Sons") consists of your license details and the terms and conditions provided by John Wiley and Sons and Copyright Clearance Center.

Your confirmation email will contain your order number for future reference.

Printable Details

License Number	5553840294762
License date	May 21, 2023

Licensed Content

Licensed Content Publisher	John Wiley and Sons
Licensed Content Publication	Wiley Books
Licensed Content Title	Absorption and Photocurrent Spectroscopy with High Dynamic Range
Licensed Content Author	Thomas Kirchartz, Thomas Christian Mathias Müller
Licensed Content Date	Jul 22, 2016
Licensed Content Pages	25

Order Details

Type of use	Dissertation/Thesis
Requestor type	University/Academic
Format	Electronic
Portion	Figure/table
Number of figures/tables	1
Will you be translating?	No

About Your Work

Title	CHEMICAL STRUCTURAL AND OPTICAL ABSORPTION PROPERTIES OF DYES EXTRACTED FROM SELECTED PLANT MATERIALS FOR DYE SENSITIZED SOLAR CELLS
Institution name	Kyambogo University
Expected presentation date	May 2023

Additional Data

Order reference number	https://doi.org/10.1002/9783527699025.ch8
Portions	Figure 8.6

Requestor Location

Requestor Location	Mr. Mohammad Tibenkana Kyambogo kampala, Central 0000 Uganda Attn: Mr. Mohammad Tibenkana

Tax Details

Publisher Tax ID	EU826007151

$ Price

Total	0.00 USD

Total: 0.00 USD

SPRINGER NATURE

Ultraviolet-Visible (UV-VIS) Spectroscopy

Author: Muhammad Sajid Hamid Akash, Kanwal Rehman
Publication: Springer eBook
Publisher: Springer Nature
Date: Jan 1, 2020

Order Completed

Thank you for your order.

This Agreement between Mr. Mohammad Tibenkana ("You") and Springer Nature ("Springer Nature") consists of your license details and the terms and conditions provided by Springer Nature and Copyright Clearance Center.

Your confirmation email will contain your order number for future reference.

Printable Details

License Number	5554130935145
License date	May 22, 2023

Licensed Content

Licensed Content Publisher	Springer Nature
Licensed Content Publication	Springer eBook
Licensed Content Title	Ultraviolet-Visible (UV-VIS) Spectroscopy
Licensed Content Author	Muhammad Sajid Hamid Akash, Kanwal Rehman
Licensed Content Date	Jan 1, 2020

Order Details

Type of Use	Thesis/Dissertation
Requestor type	academic/university or research institute
Format	electronic
Portion	figures/tables/illustrations
Number of figures/tables/illustrations	1
Will you be translating?	no
Circulation/distribution	50000 or greater
Author of this Springer Nature content	no

About Your Work

Title	CHEMICAL STRUCTURAL AND OPTICAL ABSORPTION PROPERTIES OF DYES EXTRACTED FROM SELECTED PLANT MATERIALS FOR DYE SENSITIZED SOLAR CELLS
Institution name	Kyambogo University
Expected presentation date	May 2023

Additional Data

Order reference number	10.1007/978-981-15-1547-7_3
Portions	Figure 2.3

Requestor Location

Requestor Location	Mr. Mohammad Tibenkana Kyambogo Kampala, Central 0000 Uganda Attn: Mr. Mohammad Tibenkana

Tax Details

$ Price

Total	0.00 USD

Development of a multi-source solar simulator for spatial uniformity and close spectral matching to AM0 and AM1.5

Conference Proceedings: 2011 37th IEEE Photovoltaic Specialists Conference
Author: Stephen J. Polly
Publisher: IEEE
Date: June 2011

Comparative photo-response performances of dye sensitized solar cells using dyes from selected plants

Author:
Emmanuel.O. Onah,S.U. Offiah,U.K. Chime,G.M. Whyte,Raphael.M. Obodo,O.V. Ekechukwu,Ishaq Ahmad,P.E. Ugwuoke,Fabian I Ezema

Publication: Surfaces and Interfaces

Publisher: Elsevier

Date: September 2020

Order Completed

Thank you for your order.

This Agreement between Mr. Mohammad Tibenkana ("You") and Elsevier ("Elsevier") consists of your license details and the terms and conditions provided by Elsevier and Copyright Clearance Center.

Your confirmation email will contain your order number for future reference.

Printable Details

License Number	5554280594193
License date	May 22, 2023

Licensed Content

Licensed Content Publisher	Elsevier
Licensed Content Publication	Surfaces and Interfaces
Licensed Content Title	Comparative photo-response performances of dye sensitized solar cells using dyes from selected plants
Licensed Content Author	Emmanuel.O. Onah,S.U. Offiah,U.K. Chime,G.M. Whyte,Raphael.M. Obodo,O.V. Ekechukwu,Ishaq Ahmad,P.E. Ugwuoke,Fabian.I. Ezema
Licensed Content Date	Sep 1, 2020
Licensed Content Volume	20
Licensed Content Issue	n/a
Licensed Content Pages	1

Order Details

Type of Use	reuse in a thesis/dissertation
Portion	figures/tables/illustrations
Number of figures/tables/illustrations	1
Format	electronic
Are you the author of this Elsevier article?	No
Will you be translating?	No

About Your Work

Title	CHEMICAL STRUCTURAL AND OPTICAL ABSORPTION PROPERTIES OF DYES EXTRACTED FROM SELECTED PLANT MATERIALS FOR DYE SENSITIZED SOLAR CELLS
Institution name	Kyambogo University
Expected presentation date	May 2023

Additional Data

Order reference number	https://doi.org/10.1016/j.surfin.2020.100519
Portions	figure 2

Requestor Location

Requestor Location	Mr. Mohammad Tibenkana Kyambogo Kampala, Central 0000 Uganda Attn: Mr. Mohammad Tibenkana

Tax Details

Publisher Tax ID	GB 494 6272 12

$ Price

Total	0.00 USD